# Kinetic and Surface Properties of α-synuclein:

## Investigating the Difference between Pure Peptide and Phospholipid Including Aggregates

*Irem Nasir*

Master of Science Thesis 2011

Department of Physical Chemistry
Lund University
Sweden


LUND
UNIVERSITY

# Kinetic and Surface Properties of α-synuclein: Investigating the Difference between Pure Peptide and Phospholipid Including Aggregates

**Diploma Thesis**

Irem Nasir

**Supervised by:**

Emma Sparr

Sara Snogerup Linse

Physical Chemistry Department

Lund University

Lund, Sweden

March 2011

**ABSTRACT**

α-synuclein is a protein that has been found in Lewy bodies and Lewy neurites, which are filamentous aggregates that known are as the onset of Parkinson's Disease. The purpose of this study to investigate how the presence of phospholipid vesicles affect α-synuclein fibrillation different than when α-synuclein fibrillated in buffer, hydrophobicity during the aggregation process, monitored by fluorescence spectroscopy. The surface properties of different α-synuclein aggregates further investigated by two complementary adsorption techniques; namely quartz crystal microbalance with dissipation (QCM-D) and ellipsometry. Results revealed that the presence of lipid vesicles alters the fibrillation process as monitored with non-covalent dye ANS, while lipid containing aggregates are predicted to have less hydrophobicity than the ones contain pure α-synuclein. Accelearing trend has also been seen with different lipid mixtures, possessing the same charge. It is observed that lipid to protein ratio is inversely proportional to the lag time. Adsorption is more in pure peptide aggregates, however different type of experiments need to be done to be sure of the aggregate properties.

**TABLE OF CONTENTS**

**ACKNOWLEDGEMENTS**

I would like to thank my supervisor Emma Sparr, for letting me into this project, in the beginning as a summer worker, being extremely patient with me and also helping me in every aspect. Also to my co-supervisor Sara Snogerup Linse for her great guidance and sharing her knowledge whenever I needed it. I would also like to thank to Erik Hellstrand for teaching me every instrument and the handling of the work step by step and being available whenever I needed. I kindly acknowledge Ulf Olsson for letting me in here as an Erasmus student in the very beginning and always being nice to me. Physical and Biophysical Chemistry Departments provided great environment for me to continue my research, I would like to thank to both academic and administrative staff of both departments.

I would like to thank my family for supporting me and loving me endlessly through each phase of my life. Lastly, my dearest acknowledgement goes to Mariano, who was a great support during this time and always putting up with me.

## INTRODUCTION

Parkinson's disease (PD) is the second most common neuro-degenerative disorder, after Alzheimer's disease. Clinically, it is a movement disorder that is characterized by tremor, rigidity, and bradykinesia. PD is defined by nerve cell loss in the substantia nigra and the presence there of Lewy bodies and Lewy neuritis. α-synuclein is found as large amounts inside of those Lewy bodies. The pathway of the toxicity is not known but interactions of intermediate or fibrillar species of α-synuclein with cell membrane is one of the suspected ones.

α-synuclein kinetics is a well characterized for the systems that contains the protein and the buffer. Effects of pH, temperature, ionic strength and the presence of, e.g., other proteins, nanoparticles or lipid membranes have been proved to affect the α-synuclein aggregation properties, and changes in these may lead to fibrillation [1]. Most of the studies dealing with α-synuclein-lipid interactions [2, 3] concentrate on the affinity of fibrils for unilamellar lipid vesicles and one often tries to isolate the intermediate aggregate species. The objective of this study is to investigate the surface properties of aggregated α-synuclein, and how that is affected by aggregation of the protein in the presence of lipids. The methodology of this work is different from most previous studies in that we simultaneously study changes in the aggregate properties while tracking the fibrillation kinetics without trying to isolate intermediate aggregation states. We have tried to form aggregates in presence of lipid vesicles and investigated the intermediate species on-line with the fibrillation process in simultaneously.

The system dynamics and surface properties can be tracked easily by attaching non-covalent probes to the model studied for fluorescent techniques. In this study ANS and ThT are used to track the changes in α-synuclein fibrils in buffer and when incubated with mixtures of DOPC, DOPS and CL lipids chosen as a model system. Adsoprtion techniques (i.e. QCM-D and ellipsometry) were also used to see the affinity of the model system to hydrophilic and hydrophobic surfaces.

# 1. THEORY

## 1.1 System Background

### 1.1.1 Amyloid Protein Aggregation

Folding of a polypeptide chain into specific three-dimensional structure is closely related with the energy landscape. Native state of a protein corresponds to the lowest energy of the system and it is thermodynamically stable.

The term "amyloid" implies a particular kind of highly ordered and elongated protein aggregate rich in beta sheet structure. Amyloid can be formed from many kind of polypeptide sequences, at least under some conditions. In some cases, protein misfolding can lead the system to malfunction and disease. When the amyloid proteins manage to escape all the protective mechanisms in the cell, they may form intractable aggregates either in cells or in extracellular area. Especially accumulations in brain, heart and spleen tissues of this kind of aggregated amyloid proteins lead to Alzheimer's, Parkinson's, Huntington's Disease and Type II Diabetes.

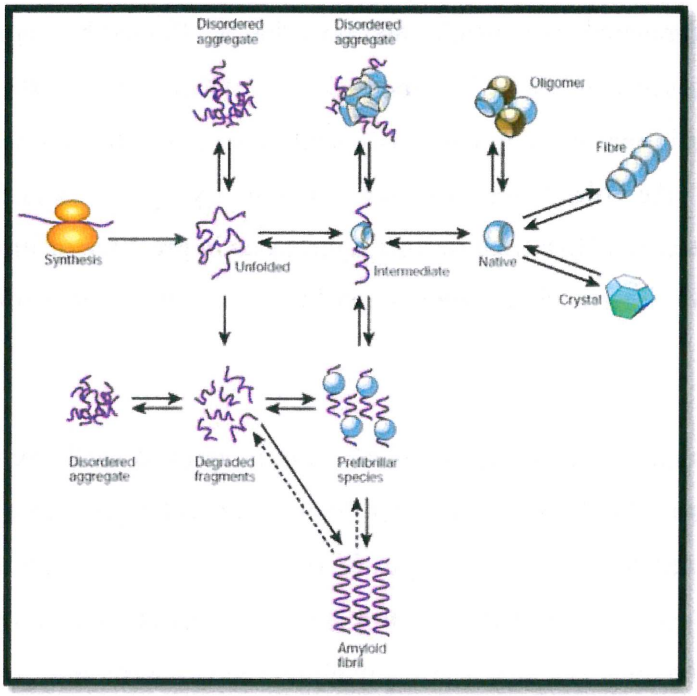


Figure 1.1 Possible structures formed by polypeptide chains [4]

The aggregated peptides have many structural properties in common. The fibrillar morphology is quite the same in most of the cases: long, unbranched and often twisted structures and a few nanometers in diameter. Furthermore, it has been discovered that amyloid fibrils are composed of beta sheets whose strands are perpendicular to the fibril axis. [5]

There are also similarities in the aggregation behavior of different peptides and proteins. The first step in amyloid formation seems to involve the formation of soluble oligomers. The research on this earliest stage using imaging techniques has revelaed small bead-like structures, often described as amorphous aggregates or micelles [4].The early structures then transform into short, thin, curly fibrillar species called "protofibrils". After that, those protofibrils assemble into mature fibrils most probably by lateral association. [4]

### 1.1.2 The Role of Lipids in Amyloid Formation

Lipid-protein interactions play an important role in many of the cellular processes such as intracellular transport, enzyme catalysis and control of membrane fusion. Lipids are small amphiphilic molecules, which means that they have both hydrophobic and hydrophilic domains. The amphiphilic character of lipids help them to self assemble in different structures, i.e. micelles, bilayers etc. Lipid bilayers can be described as the basic structural elements of the biological membranes, and it is often thought of as two-dimensional liquid providing a variety of environments. A bilayer is either in liquid or in gel phase. Short and unsaturated lipids generally have lower melting temperature due to less strong van der Waals interactions between the hydrocarbon chains [6]. Under physiological conditions, the main fraction of the phospholipid molecules in the cell membrane are in the liquid crystalline state but they can be present as "lipid rafts", which is more rigid and consist different subtypes of lipids, including cholesterol. Membane-protein interactions can be controlled by membrane's physicochemical state (solid or fluid state), or by the chemical nature of membrane lipids, chain saturation, conformation of headgroups and acyl chains as well as protein's properties.

The fibrillogenic properties of the membrane associated amyloid proteins have found to be closely related to the nature of lipids. Especially anionic phospholipids show stronger interaction with many types of amyloid peptides, and therefore likely affect fibrillation [7]. Moreover, aggregation speeds up with the degree of phosphorylation, suggesting that the phosphate groups are essential for fibril formation as found in Islet amyloid polypeptide (IAPP) [8].

Membranes composed of mixed lipids in many cases have an impact on fibrillation process, presumably both by electrostatic interactions that might lead to conformational changes in the protein, and by protein adsorption to the membrane interface leading to the accumulation of proteins. Some examples of those mixtures that have been studied together with amyloid proteins are 1,2-Dipalmitoyl-*sn*-glycero-3-phosphate (PA)/ 1,2-dipalmitoyl-*sn*-glycero-3-phosphocholine (PC), 1,2-dipalmitoyl-*sn*-glycero-3-phospho-RAC-(1-glycerol) (PG)/PC, 1,2-Dipalmitoyl-*sn*-glycero-3-phospho-L-serine (PS)/PC or PG/1,2-dipalmitoyl-*sn*-glycero-3-phosphoethanolamine (PE) vesicles with saturated or unsaturated chains.[7, 9]

### 1.1.3 Description of the Model System

The model system of our choice is the human α-synuclein protein, which is an amyloid protein mostly prevalent in presynaptic nerve terminals. α-synuclein is a major component in so-called Lewy bodies, which are characteristic to Parkinson's disease (PD). α-synuclein found in Lewy bodies is aggregated into amyloid fibrils. Lewy bodies also contain other proteins and lipids. α-synuclein containing Lewy bodies has also been found in some types of Alzheimer's disease (AD) [10]. α-synuclein contains 140 amino acids (Figure 1.2), and it adopts a random coil structure in the native state [11]. Mutations ease the folding of this protein.

**MDVFMKGLSKAKEGVVAAAEKTKQGVAEAAGKTKEGVLYVGSKTK**
**EGVVHGVATVAEKTK**
N-terminus residue 1-60: alpha helix

**EQVTNVGGAVVTGVTAVAQKTVEGAGSIAAATGFVK**
NAC region residue 61-95: beta sheets

**KDQLGKNEEGAPQEGILEDMPVDPDNEAYEMPSEEGYQDYEPEA**
C-terminus residue 96-140: unstructured

Figure 1.2 α-synuclein sequence

The lipid systems chosen for this study contain 1,2-dioleoyl-*sn*-glycero-3-phosphocholine (DOPC, will be abbreviated as PC from now on), cardiolipin and phospahtidylserine (PS). PC is a zwitterionic lipid with one negative charge on the phosphate group and one positive on the amine group, yielding an overall charge of zero. DOPC is abundant in most cell membranes. Cardiolipin is a divalent negatively charged lipid that is present in mithodcondia membrane [12]. Studies reveal that CL amount decreases by aging, emerging from lipid peroxidation in cells, which is believed to be an important factor in neuronal loss. [13] Also another membrane abundant lipid, 1,2-dioleoyl-*sn*-glycero-3-phospho-L-serine (DOPS). DOPS is an anionic and monovalent lipid, which is present in the inner monolayer of the membrane. All the lipids used in the system forms lamellar phase, which then can be dispersed as unilamellar vesicles in solution. [14]

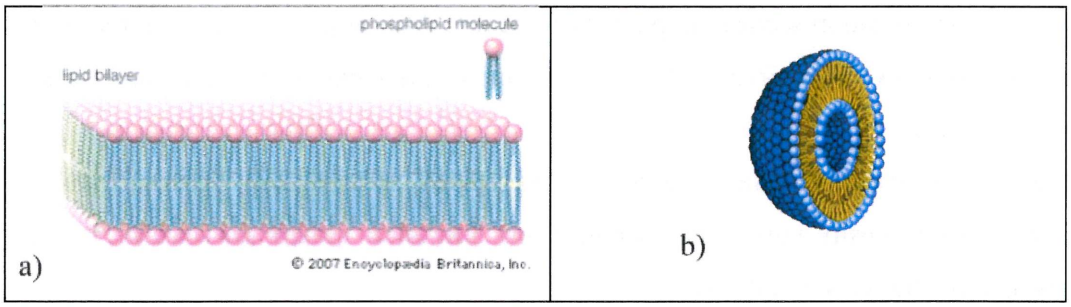


Figure 1.3 Illustrations of a) lipid bilayer b) Vesicle [15]

In this study we rather use these model systems to explore the effect of the different lipid components on protein interaction. Peptide to lipid ratio has been chosen for being reasonable considering cell environment. We use peptide/lipid ratios ranging from 1:0.078 to 1:10.

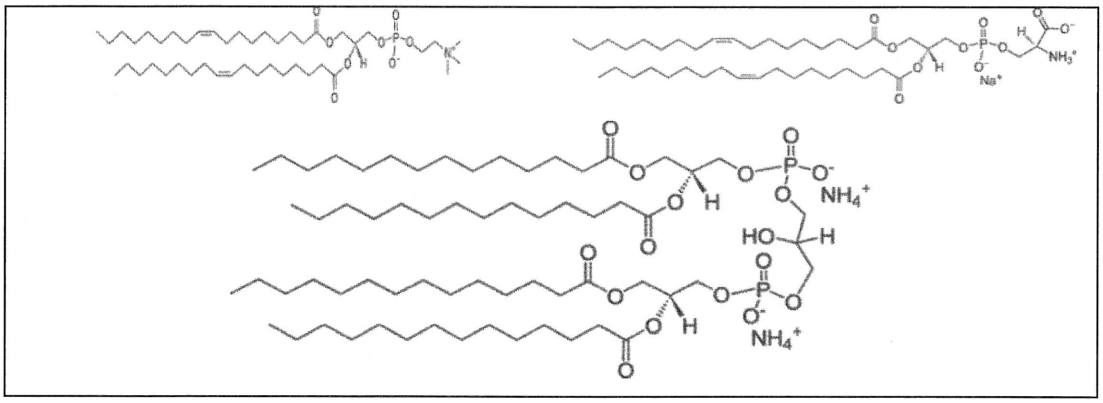

Figure 1.4 Top Left : Structure of DOPC, Top Right: Structure of DOPS, Bottom: Structure of Cardiolipin [16]

## 1.2 Experimental Methods

### 1.2.1 Fluorescence Spectroscopy

The phenomenon of emission of the light from a substance is called "luminescence". Luminescence is a result of electronically excited states and this can happen in two ways: either as fluorescence or phosphorescence. The origin of the difference in between these two categories is the nature of the excited state (i.e. singlet and triplet excited states.).

Fluorescence spectral data is generally expressed as emission spectra, having fluorescence intensity versus wavelength (nm). Emission spectra are specific to the fluorophore and the solvent used.

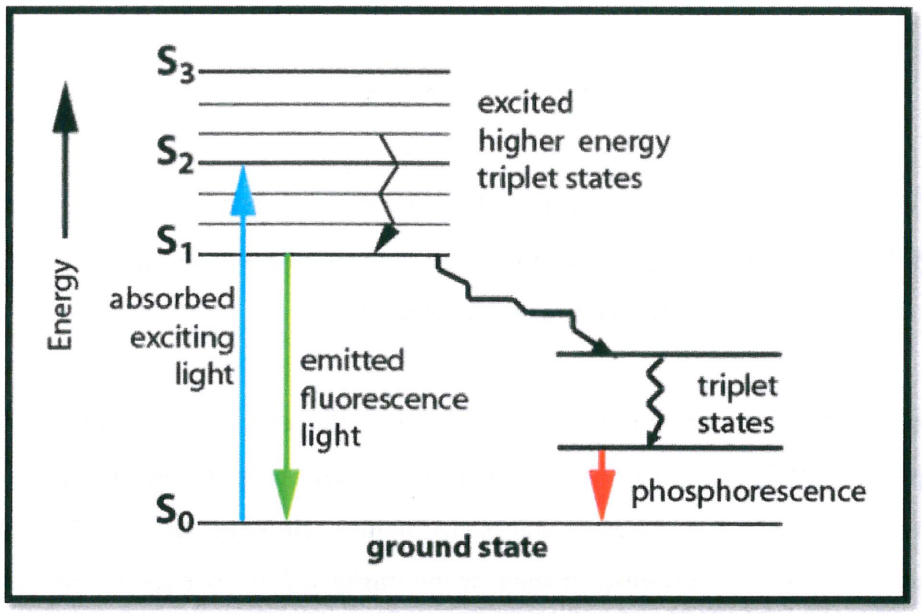


Figure 1.5 Jablonski Diagram [17]

Above shown, is a Jablonski diagram, which explains the processes that occur between absorption and emission of the light. The transitions between the levels are shown as vertical lines and the transitions occur in $10^{-15}$ s, which is too short for displacement of the nuclei (vibrational transitions, which happen in $10^{-13}$ s). This is called Frank-Condon principle. Thus, the first step of the events occurring is the electronic transition without the change in the positions of atomic nuclei. However, lifetime of the excited state ($10^{-10}$ s) is longer compared to atomic nuclei redistribution, so the second step of the sequel is the atomic nuclei displacement in order to adjust the new excited state of the electrons. Then the electrons go back to their original state, as stated above, almost instantaneously.

As a result, also can be seen from Jablonski Diagram, the energy of fluorescence is less than absorbance energy. Since the wavelength is reciprocal to the energy, fluorescence occurs at longer wavelengths than the absorbance. This is called Stokes Shift and it is also a function of solvent effects, excited-state reactions, complex formation and/or energy transfer.

Brightness of a fluorophore is defined by the quantum yield. It is basically the number of emitted photons relative to the number of absorbed photons. Substances that have quantum yield close to unity gives the brightest emissions.

$$\Phi_F = k_F / (k_F + k_{ic} + k_{is} + k_Q[Q]) = \tau_F / \tau_R \quad (1)$$

where $k_F$ is the rate of fluorescence, $k_{ic}$ is the rate of internal conversion, $k_{is}$ the rate of inter system crossing and $k_Q$ is the rate of the quenching times the quencher. $\tau_F$ and $\tau_R$ are fluorescence and radiative life times, respectively.

Fluorescent probes can be divided into two classes, intrinsic and extrinsic fluorophores. Intrinsic protein fluorescence is a natural property of aromatic amino acids, namely; tryptophan, tyrosine and phenylalanine. However most of the time, the molecules of interest are nonfluorescent or the intrinsic fluorescence is too weak for detection. In this case, fluorescence is achieved by labeling them with flourophores that have longer excitation and emission wavelengths. For this case, the fluorescence is obtained by labeling the molecule with extrinsic probes. Labeling can be covalent or non covalent.

In many studies of proteins as well as other molecules, non-covalent probes are widely used since they are extremely sensitive even to a small change in the polarity of the environment. The polarity change monitoring is important because it reveal changes in the probe molecular surrounding, which can reflect properties of the medium and attraction with lipids and other macromolecules.

In essence, polarity change originates from Stokes shift, which proposes that emission occurs at longer wavelengths than absorption. In other words, the energy of emission is always lower than the energy of absorption. In addition to the energy loss due to atomic displacement, solvent effects shift the emission to lower wavelengths due to stabilization of the excited state by the polar solvent molecules. A fluorophore generally has larger dipole moment in excited state than the ground state. Given that information, the solvent dipoles can rearrange themselves at the excited state around the fluorophore's dipole, which results as lowering the energy of an already lowered energy of the excited state as a result of solvent relaxation shifting the spectra to the longer wavelengths.

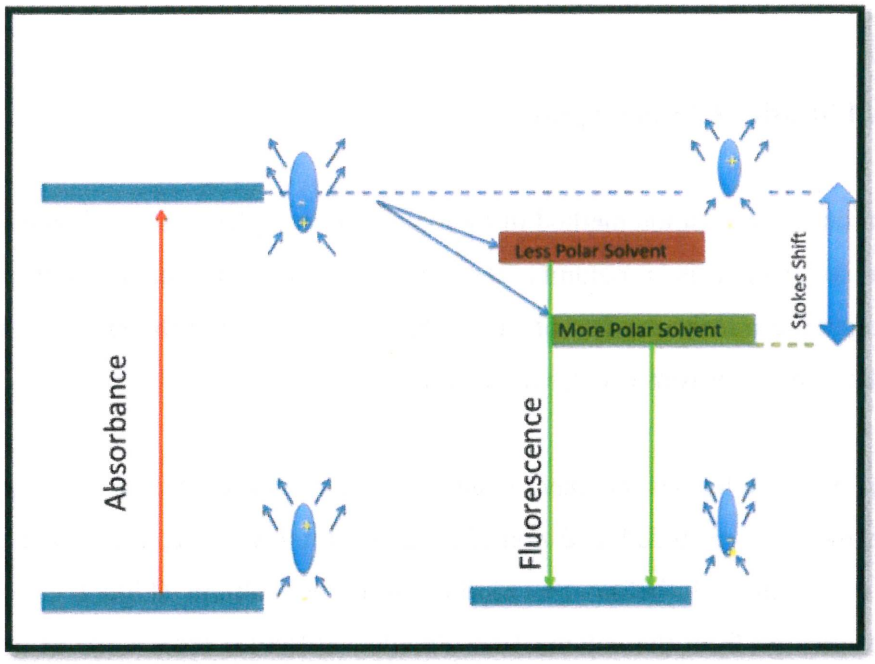


Figure 1.6 Stokes Shift and Dipole Alignment Illustration

This property of the non-covalent probes and solvent effects altogether, makes fluorescence spectroscopy perfect for monitoring the changes of the environment in protein studies, i.e. keeping track of the protein folding, protein aggregation, monitoring the conformational changes within the protein itself and ligand binding. Thioflavin T is frequently used for monitoring amyloid protein aggregation, The affinity of Thioflavin T to the cross beta sheets makes it available since the early stages of fibrillation process include lots of cross beta structures [18]. ANS binding is driven by the hydrophobic and electrostatic interactions and it monitors hydrophobic patches of the molecule examined. The peak at the spectrum shifts to lower wavelength when hydrophobicity is detected by ANS. [19]

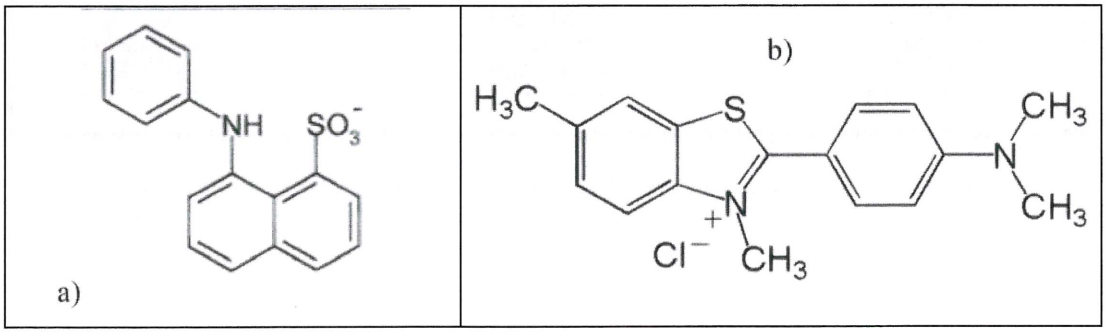


Figure 1.7 Chemical Structures of a) ANS b) ThT [18]

### 1.2.2 Gel Filtration Chromatography

Gel filtration is a separation method of biological macromolecules based on their size. Its main component is a column, containing a "chromatographic matrix". This chromatographic matrix consists of beads that have pores and the size of the pores defines the size of macromolecules to be separated.

Basically, macromolecules that have larger size than the pores cannot enter the pores, therefore they are excluded and considering the total volume, they have smaller volume to go through before the elution from the column (Figure 1.8). Large molecules emerge from the column first. Smaller molecules enter some of the pores giving a travel time throughout the column which is longer than in the previous case. Finally, the smallest molecules enter all the pores in the matrix, which elongates the times spent in the matrix, so they are eluted last.

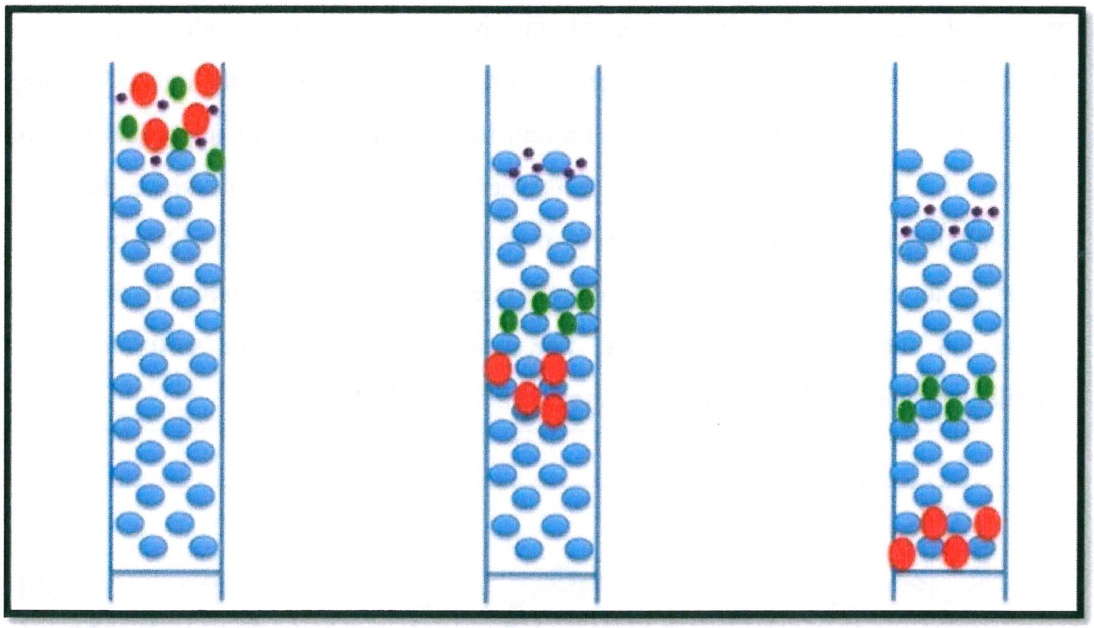

Figure 1.8 Schematic representation of gel-filtration chromatography.

As stated above, the heart of the gel filtration technique is the column, which is a glass or plastic cylinder, containing column a support. The longer column, the better

filtration, and thus better resolution. Tubing of the column should have as small volume as possible to avoid the mixing of already separated particles. Buffer is delivered to matrix by a pump with a flow rate control. Lastly, an absorbance detector in the UV wavelength range gives the absorbance of the eluting sample, and the signal is transferred to a computer for further analysis. There are commercially available column matrices designed for different fractionation ranges, defined by molecular weight range of the sample that will be purified.

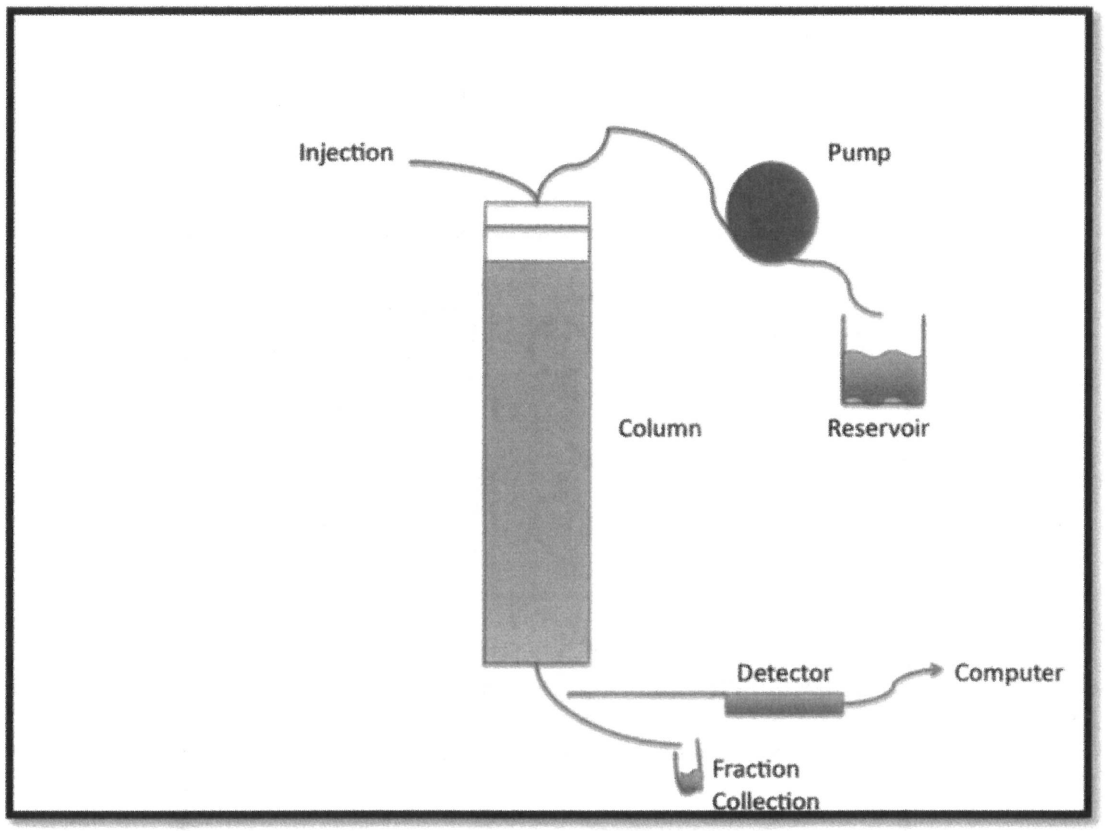


Figure 1.9 Schematic representation of chromatography equipment.

Other than being a purification method, gel filtration can also be used as buffer exchanger. The idea behind is so that, the desired buffer is already pre-equilibrated in the system and also being used as flow buffer. As a result of that, the macromolecule that is being eluted will be in the new buffer, which is in equilibrium with the column. The sample's buffer emerged from the column the latest. [20]

### 1.2.3 Quartz Crystal Microbalance with Dissipation (QCM-D)

Quartz crystal microbalance is a technique that allows characterization of thin films formed on a surface in liquid by using the piezoelectric effect in quartz. The QCM-D technique stipulates that when a quartz crystal immersed in gas or aqueous solution, it oscillates at a fundamental resonant frequency, 5 MHz. When the sample adsorbs on the crystal surface, the resonance frequency decreases in correlation with the amount of mass on the surface (Figure 1.5). QCM-D crystals are essentially gold but in most of the cases they are coated with silicon dioxide layer to demonstrate the hydrophilic surfaces. Titanium, aluminum oxide and polystyrene are also used. [21]

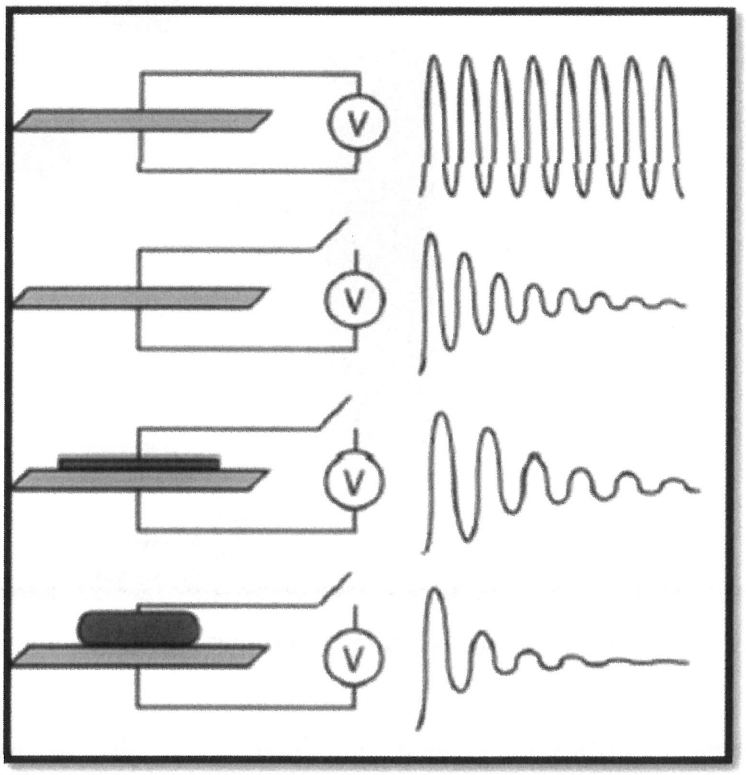


Figure 1.10 Schematic representation of frequency change with respect to the material adsorbed. [22]

QCM-D is not only able to monitor the mass of the sample adsorbed. The ability of having a dissipation monitor gives structural information about the samples being adsorbed. Dissipation means sum of the energy losses of the system per oscillation

cycle. The mass of the sample adsorbed can be found out by frequency shift, and this mass include coupled water that could vary between 10% and 90%. A film formed of molecules that extend out in the solution gives a high dissipation while a compact film at the surface gives low dissipation.

If the adsorbed mass is distributed evenly and as a compact film that give hardly any dissipation, the frequency shift ($\Delta f$) and mass per unit surface ($\Delta m$) can be correlated by Sauerbrey model.

$$\Delta m = -\frac{C \cdot \Delta f}{n} \tag{2}$$

where C is the mass sensitivity constant, 17.7 ng/cm$^2$Hz at resonant frequency 5 MHz, and $n$ is the overtone number ($n$ = 1,3,5,7,9,11,13).

In some cases, the adsorbed molecules have a high capacity of coupling water, and the film is then called "viscoelastic". In such cases, large dissipation shift and spreading between overtones occurs. For these cases, the Sauerbrey relation is not valid anymore. Typically, if the dissipation value reaches above 10-$^6$ per 10 Hz, then the film contain too much coupled solvent to fulfill the conditions for the Sauerbrey model. The viscoelastic properties such as density, elasticity and thickness of the adsorbed layer can be correlated with frequency shift by Kelvin-Viogt model. This model can be described as;

$$G^* = G' + iG'' = \mu_1 + i2\pi f\eta_1 \tag{3}$$

where $G^*$ is complex shear modulus, $G'$ is the storage modulus and $G''$ is the loss modulus. The software from Q-Sense, "*QTools*" correlates dissipation and frequency shift and estimates the viscoelastic properties of the film formed.[4, 22, 23]

### 1.2.4 Ellipsometry

Ellipsometry is a surface technique that is complementary to QCM-D. It is used for measuring the thickness, the adsorbed amount and other properties of thin layers at an interface. The setup consists of a light source that generates light, which is then polarized linearly by a polarizer. The polarized light enters a compensator where it is elliptically polarized by generating a phase shift. Then the light falls on the sample and after reflection it goes to analyzer and detector, respectively.

The data analysis is based on complex reflectance ratio, which consists of delta ($\Delta$) and psi ($\Psi$) parts. Delta is the phase shift from the incident light and psi is the amplitude ratio. By proper modeling, those two parameters can give information about the thickness of the adsorbed layer and optical constants of the sample. The fundamental equation of ellipsometry is shown below;

$$\rho = \frac{R^P}{R^S} \tag{4}$$

where $\rho$ is complex reflectance ratio (of $R_p$ and $R_s$, amplitude of p-polarized and s-polarized light, respectively) can be decomposed into,

$$\rho = \tan\Psi e^{i\Delta} \tag{5}$$

Ellipsometric techniques can be divided into two groups, namely single wavelength ellipsometry and spectroscopic ellipsometry. Single wavelength ellipsometry (SWE) employs a laser light source in a fixed wavelength. SWE instruments are suitable for measuring the thickness and refraction index of one transparent layer on a substrate. Spectroscopic ellipsometry (SE), on the other hand, spans a broad range of wavelengths. This property of SE made it difficult to be used in the early days because focusing of the beam on a small spot was quite challenging. The benefit of SE is that it gives an access to large number of physical properties by measuring the complex refractive index.

The essence of the ellipsometry measurements includes a substrate, mainly silicon dioxide ($SiO_2$) and the adsorbent. Silanized surfaces are also used. When the adsorbent is injected in solution, polarizer and analyzer adjust themselves such that they maintain the minimum intensity. [24]

## 2. MATERIALS and METHODS

### *Peptide purification*

The peptide used in this work is α-synuclein, which has 140 amino acid residues. Human α-synuclein was obtained from the Biochemistry Department, Lund University, where it was produced from a plasmid in *Escherichia coli* and purified using anion exchange chromatography. The protein was stored at -20°C until needed.

Prior to each experiment, alpha-synuclein was purified by a Superdex 75 column in 10 mM MES (2-(*N*-morpholino)ethanesulfonic acid), pH 5.5 buffer and monomers in solution were collected into Eppendorf tubes and kept on ice. Concentration of the monomers was determined from the absorbance of the peak in the FPLC chromatogram and the value from UV-Absorbance of the collected fraction using an extinction coefficient of 5776 $M^{-1}cm^{-1}$ at 280 nm.

### *Vesicle Preparation*

DOPC, DOPS and cardiolipin were obtained from Avanti Polar Lipids (Alabaster, Alabama). Stock solutions were prepared in chloroform:methanol 9:1, volume:volume. Thin films composed of the lipids then deposited in glass tubes from the solution and dried under slow nitrogen flow and continuous rotation of the vial. Remaining chloroform and methanol was then dried in vacuum over night. After, 10 mM pH 5.5 MES buffer was added to the lipid film, giving a final concentration of approximately 0.5 mM. The dispersed multilamellar aggregates were then sonicated with microtip sonication having a 40% duty cycle until no turbidity was detected by naked eye to obtain small unilamellar vesicles (SUVs)

### *Dynamic Light Scattering (DLS)*

Vesicle size determination was carried on using Zetasizer Nano ZS (Malvern Instruments Ltd., UK) at temperature of 25°C and 3 sequential scans were performed to get a good statistics of data.

***On-line Measurements with Plate Reader***

After collection of fresh monomers of alpha synuclein on ice, the solutions were distributed with desired concentration in a 96 well non-treated black polystyrene plate with transparent bottom (Corning). In the present experiments, the wells contained 100 µl of either peptide alone, peptide mixed with lipid vesicles or lipid vesicles alone – to have a control of the experiments. The peptide concentration was always set to 2.3 µM, and the lipid concentration was 23 µM unless stated otherwise. The plate was sealed to avoid the evaporation. The experiment was started by inserting the plate into (Fluostar Omega, BMG Labtech) the plate reader at 37°C and starting orbital shaking at a rate of 100 rpm in five-minute cycles. ANS fluorescence was measured before each 5 minute shaking interval, right after an excitation of 360 nm. After shaking for 5 minutes, ThT fluorescence was measured at the emission wavelength of 480 nm with an excitation wavelength of 440 nm.

During the experiment, at different chosen time points, selected samples were collected for further analysis by fluorescence spectroscopy. In order to do that, the plate reader was stopped (as short as possible to avoid any interference with the measurement). To get a homogeneous sample, 100 µl of buffer was added to the wells to be taken, and the sample was pipetted into Eppendorf tubes prior to re-insertion of the plate.

***Fluorescence spectroscopy***

Fluorescence spectroscopy measurements were carried out in the spectrometer (Cary Eclipse, Varian) by using excitation and emission slits of 5 with voltage varying between 600 and 1000 W, depending on the sample. 10 mm. quartz cuvettes containing the solution from one well (peptide, peptide and lipid, lipid) and fluorescent probe (ANS or ThT) were inserted into the fluorescence spectrometer. The spectra were recorded over a wavelength range of 400 to 600 nm after excitation at 350 nm for ANS, and over a wavelength range of 460 to 550 nm with an excitation at 420 nm for ThT. At least 3 sequential scans were performed to improve data statistics. The temperature was set to be 25°C before each experiment and equilibrated for 5 minutes and small magnetic beads were used for continuous stirring.

### *QCM-D Measurements*

QCM-D experiments were carried out by Q-Sense E4 (QSense), which consisted of four thermally insulated cells. The sensor crystals (Q-Sense, Gothenburg, Sweden) with a layer of $SiO_2$ and 5 MHz fundamental resonance frequency were cleaned by SDS and rinsed with MilliQ water, ethanol, respectively. The crystals were then dried under nitrogen flow and vacuumed. This procedure was followed by air plasma cleaning (Harrick Scientific Corp., model PDC-3XG) for 5 minutes, before each experiment.

Continuous flow of bulk liquid was provided by a peristaltic pump. All experiments were performed at 25°C.

### *Ellipsometry Measurements*

Ellipsometry measurements were performed by using an automated Rudolph Research thin-film ellipsometer operating at 4015 Å wavelength. A trapezoidal cell of 5 ml was used with a magnetic stirrer operating at 300 rpm. The temperature was set to be 25°C. The teflon tubes were used to adjust the flow inside the cell operated by a peristaltic pump.

$SiO_2$ coated substrates were rinsed with ethanol and MilliQ water, respectively. They had been cleaned by the procedure that is described above. Silanized surfaces were only rinsed with ethanol and MilliQ and dried under nitrogen flow.

In prior to each experiment, the optical properties of the sample were determined by measuring in different ambients, namely air and water.

Adsorbed amount was calculated by using the formula above

$$\Gamma = \frac{(n - n_0)d}{dn/dc} \tag{6}$$

where $n_0$ is the refractive index of the bulk solution ($n_0$=1.34) and $dn/dc$ is the refractive index change with respect to concentration ($dn/dc$ = 0.141) [25]

# 3.RESULTS

## 3.1 Methodology

Amyloid formation goes from the monomeric peptide to large fibrillar aggregates containing thousands of peptides. The field of amyloid research is very much focused on isolating specific intermediate oligomeric species that are present between the monomeric and the fibrillar states. This assumes that the intermediate oligomers stable and long-lived enough to make it possible to isolate them. An alternative way of looking at the amyloid formation is to study it as an aggregation process, where many intermediate structures co-exist and vary over time. The approach followed in this study is to study the amyloid formation process as a function of time, and defining the intermediates with respect to their position along aggregation kinetics trace. This approach includes taking out samples along the pathway and investigating them with appropriate techniques. The position of the intermediate is obvious since the kinetics of the system is well defined and reproducible [26]. We study the intermediates as well as the initial and final states by means of biding to two different fluorescent probes, ANS and ThT.

The aggregation kinetics followed by ThT and ANS is used to determine surface hydrophobicity. From the combination of these measurements, it is possible to follow and define the aggregation kinetics by ThT and determine the hydrophobicity of the intermediate state (whose position was determined by the kinetic measurements) anywhere along the fibrillation curve (i.e. half of the lag time, early elongation, after fibrils are formed etc.) by probing it with ANS.

## 3.2 Following Peptide Aggregation by Fluorescent Probes: α-synuclein fibrillation Pure Peptide Case

### 3.2.1 Aggregation Kinetics by Plate Reader

All the experiments described below were carried out at 100 rpm orbital shaking rate at 37°C. The ANS probe was excited at 355 nm and the emission was measured at 460 nm and 520 nm. ThT probe was excited at 440 nm and the emission was measured at 480 nm. The kinetics was followed for 45 hours.

Figure 3.1 shows a selected kinetic trace from one experiment, with a typical sigmoidal behavior of the fibrillation process monitored by ThT binding. Note that the kinetic traces were taken from the same experiment, showing four replicates of the same batch.

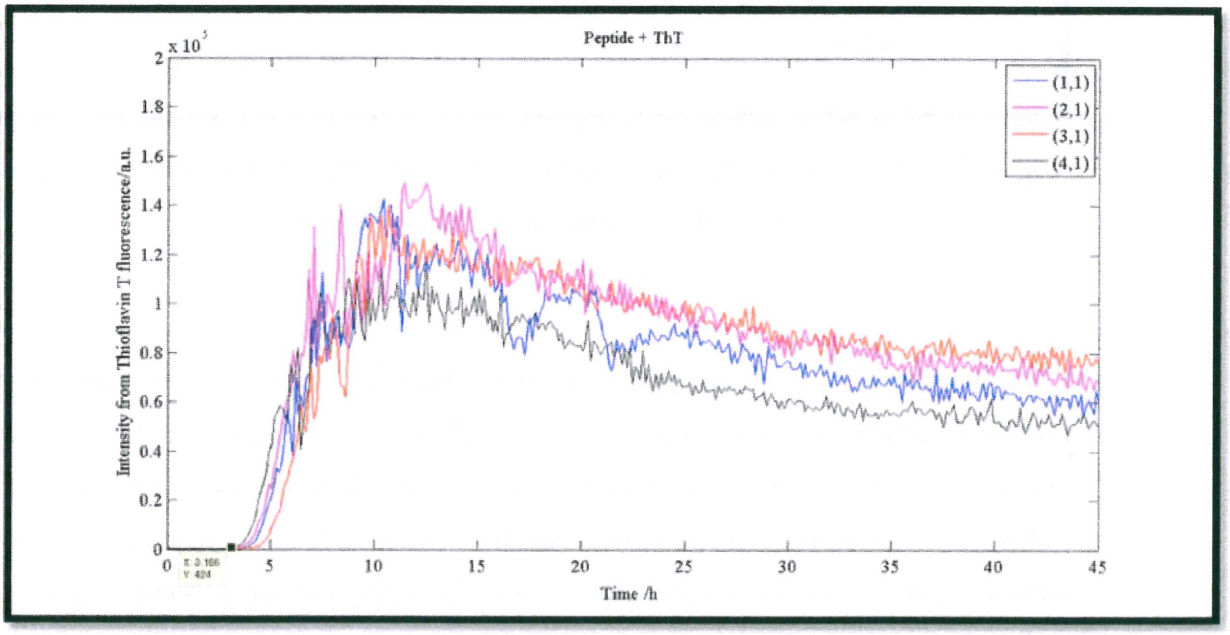


Figure 3.1 ThT Monitored Fibrillation Curve of Peptide in 10 mM pH = 5.5 MES Buffer at 480 nm. Note that Peptide : ThT Ratio is P:T = 1.15:1

The aggregation process was also followed by ANS fluorescence simultaneously to the ThT experiments, A typical set of data are shown in Figure 3.2. It is noted that the ANS intensity increases after a period of incubation. From this it is possible to measure a lag time similar to what is done for ThT. ANS fluorescence was measured

both at 460 and 520 nm. Same trends were observed in both wavelengths, except for a lower intensity at 520 nm.

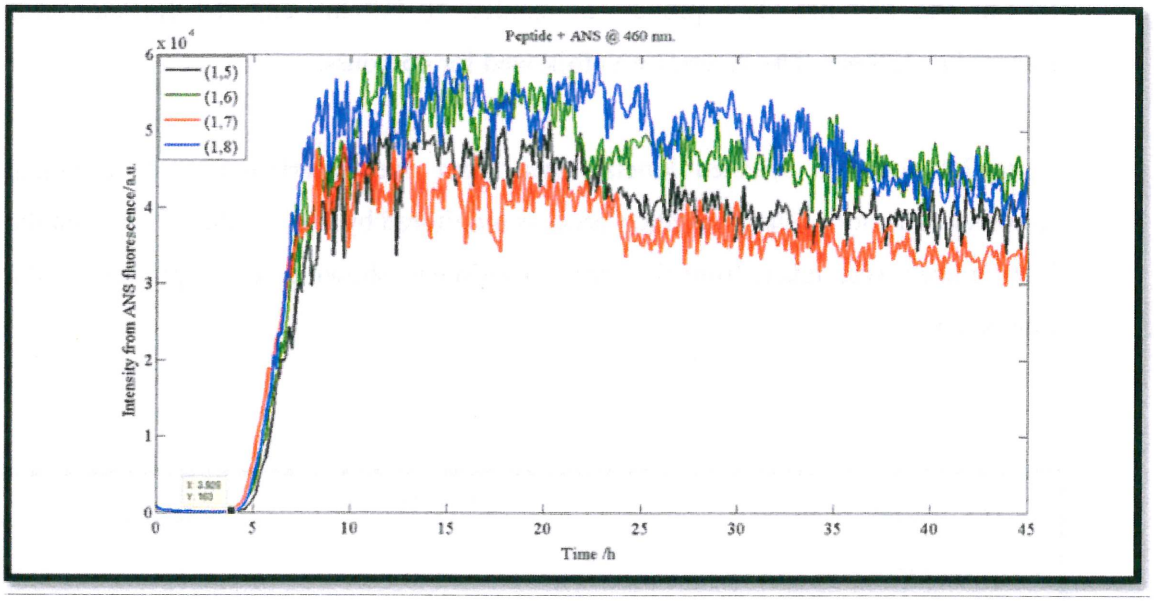


Figure 3.2 ANS Monitored Fibrillation Curve of 23 μM Peptide in 10 mM pH = 5.5 MES Buffer with 1 μM ANS at 460 nm

Table 3.1 shows experiments performed throughout the study time. It shows the peptide concentration in each well, peptide to ThT molar ratio, peptide to ANS molar ratio and lag times. Lag times are defined after normalizing the data by the lowest intensity and taking the time point when the intensity is 10% of the final value. Four wells of each sample were used. Out of total 28 wells, ThT probe gave only two outliers, which had a lag time more than 2 times longer compared to the rest of the samples with the same composition in the same experiment. In the experiments with the ANS probe, there was no outlier. The outliers are marked in Table 3.1. Results yielded an average ThT lag time to average ANS lag time ratio of 0.97 with a standard deviation of 0.1. Although the peptide concentration is the same in all experiments, the measured lag times are different. This is most probably caused by impurities in the solution and/or pipetting errors.

Table 3.1 Experimental Data from Plate Reader Measurements of 23 μM α-synuclein Fibrillation, Peptide:ThT = 1.15:1 and Peptide:ANS = 23:1

| Experiment Nr. | Lag Time (ThT) | Lag Time (ANS) | Lag time (ThT)/Lag time (ANS) |
|---|---|---|---|
| 1 | 7.7±0.6* | 7.3±0.4 | 1.1 |
| 2 | 7.5±0.4 | 7.5±0.5 | 1.0 |
| 3 | 7.9±0.3 | 7.6±0.4 | 1.1 |
| 4 | 5.8±1.0 | 7.6±1.2 | 0.8 |
| 5 | 4.8±0.4 | 5.2±0.2 | 0.9 |
| 6 | 10.6±0.4 | 9.6±0.3 | 1.1 |
| 7 | 5.8±0.2* | 7.2±0.5 | 0.8 |

From the data in Table 3.1 it is concluded that ANS and ThT intensity increases simultaneously, likely when peptide starts to fibrillate. The ratio between the lag times measured from the ThT to ANS fluorescence, is close to 1 with a small standard deviation. It is therefore concluded that the change in polarity as measured by ANS coincide with the stacking of β-sheets as detected by Thioflavin-T.

### 3.2.2 Determining the Hydrophobicity of the peptide monomer and the peptide aggregates

As explained in the methodology section, samples were picked out at selected time points and ANS or ThT spectra were recorded on a fluorescence spectrometer. The ANS fluorescence gives information on the polarity of the probe environment.

Excitation wavelength of ANS was chosen to 350 nm and emission was measured at wavelengths between 400 nm and 600 nm for most samples. In Figure 3.3 the observed overall intensity of both ThT and ANS increase over time. Another trend is a shift in the emission maximum for ANS from approximately 520 nm to 480 nm. The shift and change in ANS intensity indicate a change in aggregate hydrophobicity. However in part b, ThT does not give a clear interpretable spectrum as ANS but still increment of the intensity upon fibrillation is observable. The only exceptions to this are found for samples that had been fibrillated over many hours and eventually subjected to evaporation. The time points are defined as fraction of the lag time to enable comparisons between different experiments.

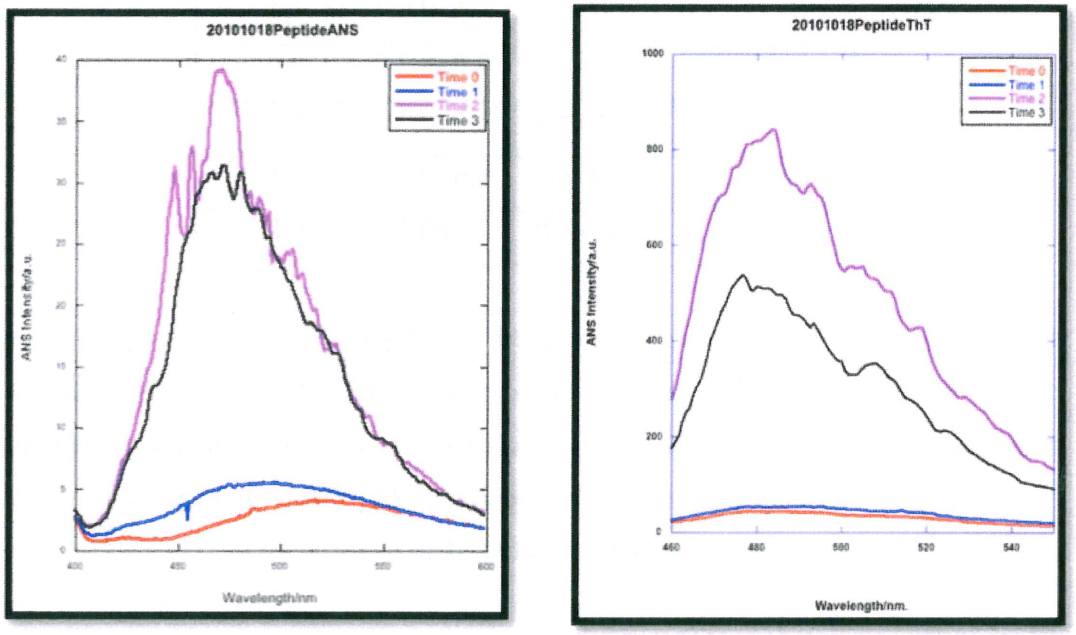


Figure 3.3 a) ANS spectrum of 2.3 μM Peptide and 3 μM ANS with excitation and emission slits of 5. First two time points are during lag time (initial and 60% of lag time respectively) and the last two points are after fibrillation. b) ThT spectrum of 2.3 μM Peptide and 40 μM ThT with excitation and emission slits of 5. First two time points are during lag time (initial, 60% of lag time respectively) and the last two points are after fibrillation.

One observation made during the studies was that, at later time points when fibrils start to form, the spectrum includes more scattering. This brings out the complexity of picking out a homogeneous sample. To overcome this problem, latter experiments were performed with duplicate samples, especially with fibrillated samples and averaged in both intensity and wavelength. In order to avoid instabilities arising from the sample state (temperature, fibrils etc.) 3 sequential scans were performed and averaged. Stirring by using small magnetic beads into quartz cells was done to provide homogeneous mixing in the sample (important especially in fibrillated samples).

Table 3.2 shows the results from 5 experiments measuring ANS spectra at different time points along the aggregation process. The shift from monomer to fibrils is significant; however the shift seen for intermediate species are not significant. Although it is not completely confirmed, a shift to lower wavelengths is seen, suggesting that intermediate species have hydrophobic patches to a small extent.

Table 3.2 Collected Fluorescence Spectroscopy Results for α-synuclein Fibrillation

| **Experiment Nr.** | **Peptide Concentration (μM)** | **Peptide : ANS** | **Corresponding Wavelength of Maximum Intensity (nm)** | **Position Along Fibrillation** |
|---|---|---|---|---|
| 1[i] | 2.29 | 0.76:1 | 526 | 0% |
| | | | 526 | 26% |
| | | | 526 | 60% |
| | | | 486 | 100% |
| | | | 480 | 100% |
| 2[ii] | 2.29 | 0.76:1 | 524 | 0% |
| | | | 488 | 26% |
| | | | ca. 470 | 60% |
| | | | ca. 470 | 100% |
| 3 | 2.29 | 0.76:1 | 520.3 | 0% |
| | | | 473.4 | 100% |

| | | | | |
|---|---|---|---|---|
| 4 | 2.29 | 0.76:1 | 510<br>470 | 0%<br>100% |
| 5 | 2.29 | 0.76:1 | 488<br>474 | 0%<br>100% |

[i] Scattering at later time points and too high intensity

[ii] Approximate values due to strong scattering.

### 3.2.3 Lipid Control Experiments

Before describing the results obtained for peptide aggregated in the presence of lipid vesicles, the control experiments for lipid vesicles in buffer are described. These experiments were performed in order to study how the presence of lipids affect the fluorescence of the ANS and ThT probes. Experiments were planned such that the lipid concentration was kept the same and instead of diluting it with peptide solution, diluted in buffer. Three different lipid system were studied, PC:CL, PC:PS and PC alone, and control experiments performed for all.

Figure 3.4 shows ANS spectra obtained for PC:CL vesicles at different time points. Those lipid samples are the ones collected from the plate, so they are in the same conditions as peptide (temperature, shaking etc.) There is no change in either intensity or corresponding wavelength of maximum intensity, indicating that lipids have no effect on fibrillation process (in terms of contributing intensity).

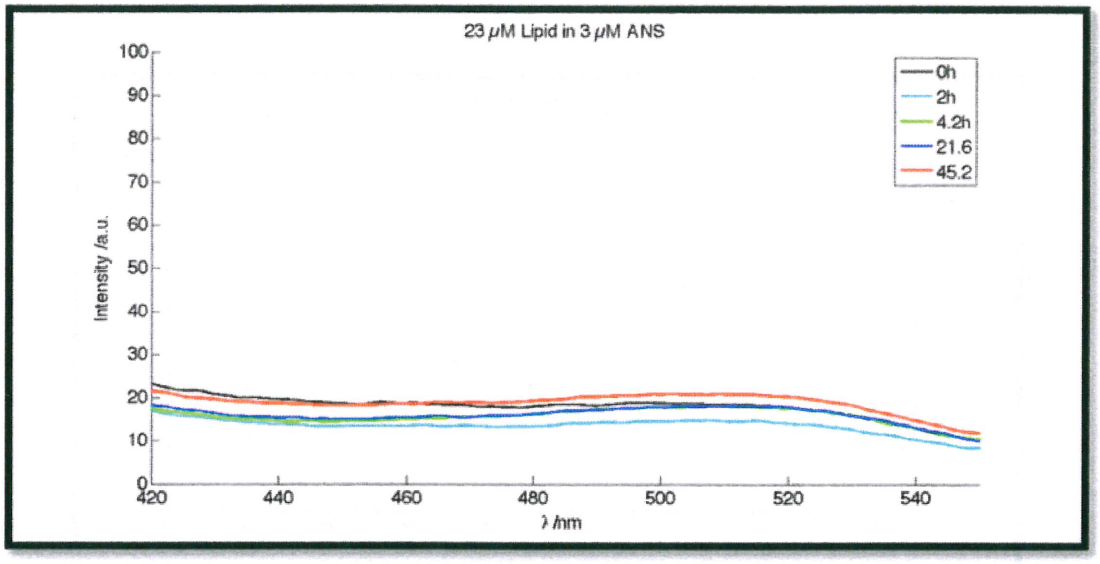


Figure 3.4 DOPC/CL in ANS Spectrum.

Figure 3.5 below shows ThT spectra probed for the lipid sample. As explained above, they also were in the same conditions as peptide and taken from the same experiment mentioned in Figure 3.4.

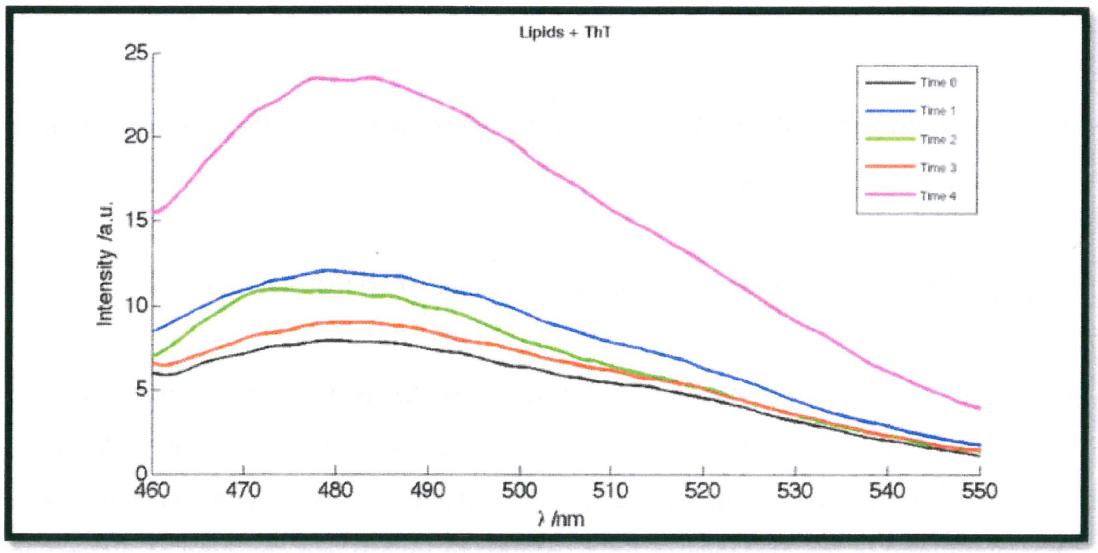


Figure 3.5 DOPC/CL in ThT Spectrum

There is no change in intensity coming from lipid vesicles, which had also been observed in plate reader experiments. Figure 3.6 below shows the intensity over time and it is clear that compared to protein incubated in buffer or protein incubated in presence of lipids, the intensity is very low.

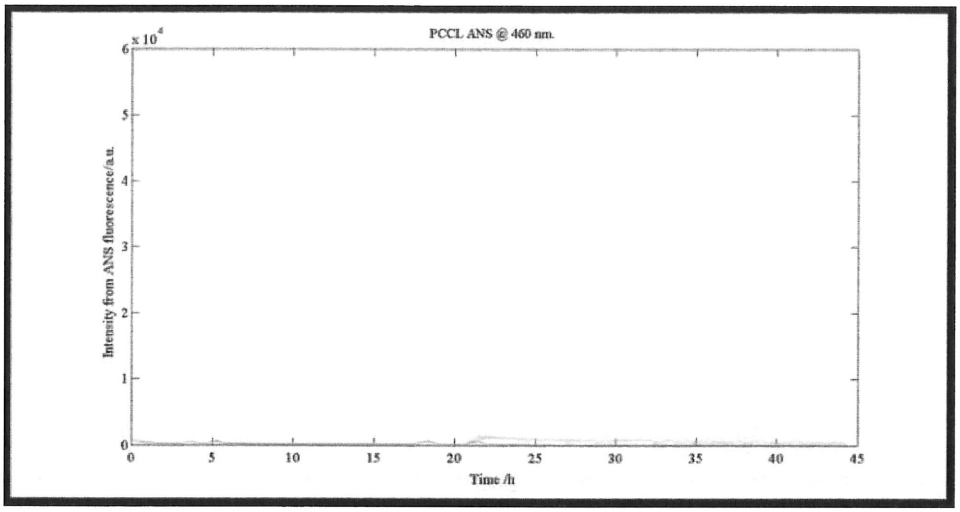


Figure 3.6 DOPC/CL in ANS scanned over 45 hours.

Similar results were obtained also for PC:PS vesicles, giving no significant change of intensity or shift in maximum emission at different time points. The plate reader results of that system also show low intensity both for ANS and ThT probes.

### 3.2.4. Following Peptide Aggregation by Fluorescent Probes: Peptide α-synuclein Incubated with Lipid vesicles

#### *Aggregation Kinetics,* α-synuclein in the presence of DOPC:CL vesicles

Essentially, the same protocol was followed in the plate reader experiments as described above. The only difference was so that a solution of lipid unilamellar vesicles were mixed with the peptide solution at the beginning, and fibrillation was thus monitored in the presence of lipid vesicles to investigate any kind of difference from the peptide fibrillation in pure buffer.

Here, the majority of the experiments were performed for the lipid system PC and CL. The data obtained from 7 experiments are presented in Table 3.3. The results yielded an average ThT lag time to average ANS lag time ratio of 2.0 with a standard deviation of 1.6. When comparing the lag time obtained from ThT fluorescence, we

first note that data are very scattered. The ratio between the lag time for peptide aggregating in the presence of lipid and the lag time for peptide aggregating alone is 1.0±0.7. Due to the large standard deviation it is not possible to judge whether the presence of charged vesicles affect the aggregation kinetics based on the ThT data.

Table 3.3 Experimental Data from Plate Reader Measurements of 23 μM α-synuclein Fibrillation in Presence of 230 μM PC:CL Unilamellar Vesicles – ThT (Peptide:ThT = 1.15:1) Probe at 480 nm

| Experiment Nr. | Lag Time (ThT) | Lag time (Peptide+Lipid)/ Lag time (Peptide + Buffer) (ThT) |
|---|---|---|
| 1 | 16.7±2.8 | 2.2 |
| 2 | 4.9±0.5 | 0.7 |
| 3 | 2.6±0.4 | 0.3 |
| 4 | 2.6±0.9 | 0.4 |
| 5 | 9.8±2.1 | 2.0 |
| 6 | 12.3±5.0* | 1.2 |
| 7 | 2.4±0.5 | 0.4 |

Table 3.4 shows the corresponding data obtained from measurements of ANS fluorescence. The ratio between the lag time for peptide aggregating in the presence of lipid and the lag time for peptide aggregating alone is 0.6±0.2. Data here is less scattered compared to Table 3.3, probably because of samples with ANS had less

evaporation. From the data it can be concluded that when lipids are present, ANS probed fluorescence gives shorter lag time

Table 3.4 Experimental Data from Plate Reader Measurements of 23 μM α-synuclein Fibrillation in Presence of 230 μM PC:CL Unilamellar Vesicles – ANS Probe (Peptide:ANS = 23:1) at 460 nm

| Experiment Nr. | Lag Time (ANS) | Lag time (ThT)/Lag time (ANS) | Lag time (Peptide+Lipid)/Lag time (Peptide + Buffer) (ANS) |
|---|---|---|---|
| 1 | 3.0±0.5 | 5.6 | 0.4 |
| 2 | 6.0±1.1 | 0.8 | 0.8 |
| 3 | 2.6±0.3 | 1.0 | 0.3 |
| 4 | 3.3±0.8 | 1.3 | 0.4 |
| 5 | 3.4±0.1 | 2.9 | 0.7 |
| 6 | 7.2±1.8* | 1.7 | 0.8 |
| 7 | 2.8±0.5 | 0.9 | 0.4 |

*Outlier

Each sample was studied in four wells for the sake of reproducing the data. Out of total 28 wells, the ThT and ANS probe gave only one outlier, which had a lag time more than 2 times of the rest in the same experiment, marked above. The large spread in the date might be explained by evaporation effects since ThT samples are placed in the first four column of the plate, which is heated from left to right.

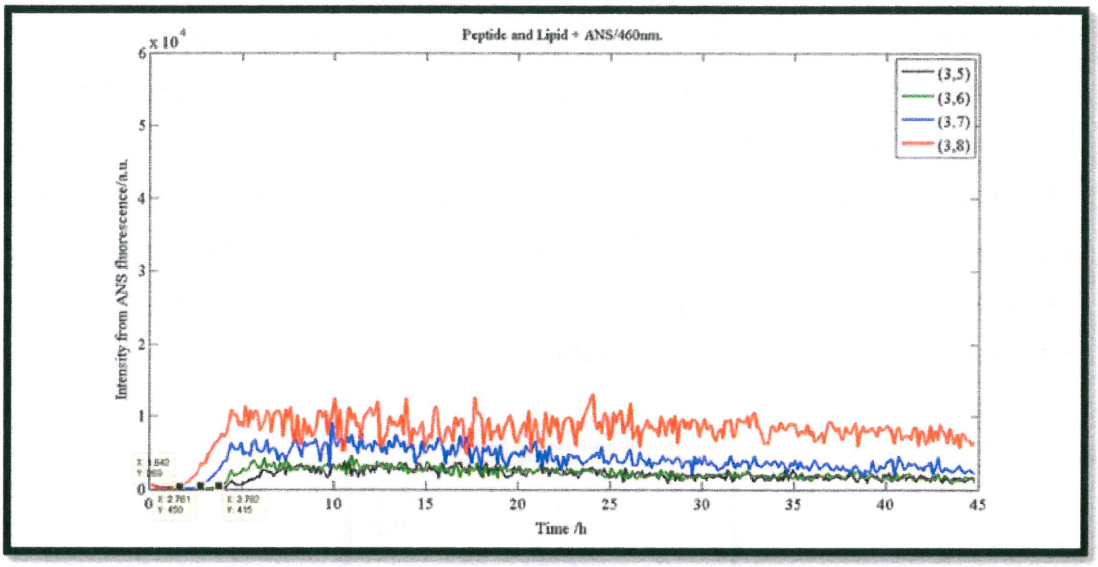


Figure 3.7 ANS Monitored Fibrillation Curve of 23 μM Peptide in presence of DOPC/CL (14 mol% CL) lipid vesicles at 460 nm. Peptide : Lipid ratio is 1:10

Figure 3.7 show a typical set of data for ANS fluorescence at 460 nm as a function of time. The most obvious difference from the situation when there is no lipid present (see Figure 3.2) is that the fluorescence intensity is much lower when lipids are present. Comparison of 7 experiments show that the ANS intensity at 460 nm is on average 2.5 times lower when lipids are present. The observation is significant as the amount of peptide and ANS is the same in these samples. Still, the fingerprint of fibrillation, sigmoidal curve is observed here as well. In this case, an acceleration of the lag time is a clear trend.

***Fluorescence Spectroscopy study of ANS and ThT fluorescence; α-synuclein in the presence of DOPC:CL vesicles***

As mentioned before, fluorescence spectroscopy experiments were performed to detect the hydrophobicity of the environment. In this special case it is much more important because it might indicates how much lipid vesicles interfere with the fibrillation process

The same procedure as described above was followed during the experiments with peptide with lipids. Samples were taken out from the wells at selected time points and

the emission spectra were recorded. The trends are rather similar to peptide in buffer, in that the overall ANS intensity increases and there is a shift in maximum. However, the intensity is in general lower and there is less scattering at late time points. There is also a slight difference in the position of the maximum intensity. For the pure peptide, there was a shift from 510 to 470 nm during the aggregation process. In the presence of lipids, the corresponding shift goes from 490 to 470 nm. The latter observation is not completely reproducible.

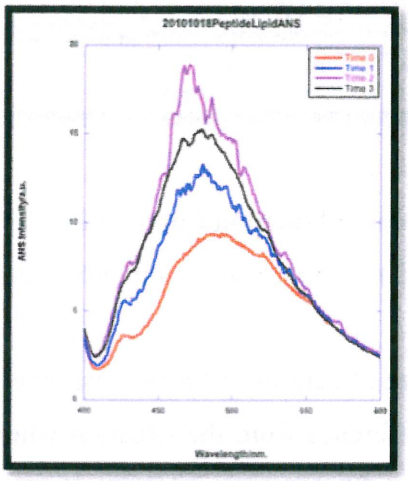


Figure 3.8 ANS spectrum of 2.3 μM Peptide incubated with 23 μM DOPC/CL in 3 μM ANS. Note that Time 0 is the initial measurement while Time 1 is the measurement at 45$^{th}$ hour.

Figure 3.8 exemplify of the observation described above: The intensity is lower and the scattering is less compared to the samples with only peptide in buffer, and the wavelength shift is slightly different. The shift in ANS emission maximum for all experiments on α-synuclein fibrillation in the presence of DOPC/CL vesicles are summarized in Table 3.5. A notable observation is that monomers in buffer give a maximum around 510 and when monomers are mixed with lipid vesicles, it shifts to lower wavelength (ca. 490 nm) while pure lipid vesicles of DOPC and CL give maximum intensity around 525 nm.

Table 3.5 Fluorescence Spectroscopy Data of α-synuclein and PC:CL incubated together

| Experiment Nr. | Peptide Concentration [μM] | Peptide : ANS | Corresponding Wavelength of Maximum Intensity [nm] | Position Along Fibrillation |
|---|---|---|---|---|
| 1 | 2.29 | 0.76:1 | 492.7 | 0% |
| | | | 479.3 | 26% |
| | | | 492.6 | 60% |
| | | | 479.3 | 100% |
| | | | 476.8 | 100% |
| 2 | 2.29 | 0.76:1 | 489.6 | 0% |
| | | | 479.2 | 26% |
| | | | 470.8 | 60% |
| | | | 478.1 | 100% |
| 3 | 2.29 | 0.76:1 | 496.8 | 0% |
| | | | 473.4 | 100% |
| 4 | 2.29 | 0.76:1 | 507.2 | 0% |
| | | | 472.9 | 100% |
| 5 | 2.29 | 0.76:1 | 510 | 0% |
| | | | 480 | 100% |

***The effect of lipid concentration on aggregation Lag Time***

The variation in lag time could be due to several factors as explained before. In order to see how the lag time dependence on the amount of charged lipid vesicles, another experiment on the plate reader was performed. 6 replicates of each concentration of lipid vesicles were monitored both by ANS and ThT. The experiment based on 1:10 peptide:lipid ratio and went down until 1:0.078 ratio. The results are summarized in Figure 3.9 In both cases, a clear decay of lag time with increasing lipid amount is seen. The difference is more pronounced in the ThT measurements.

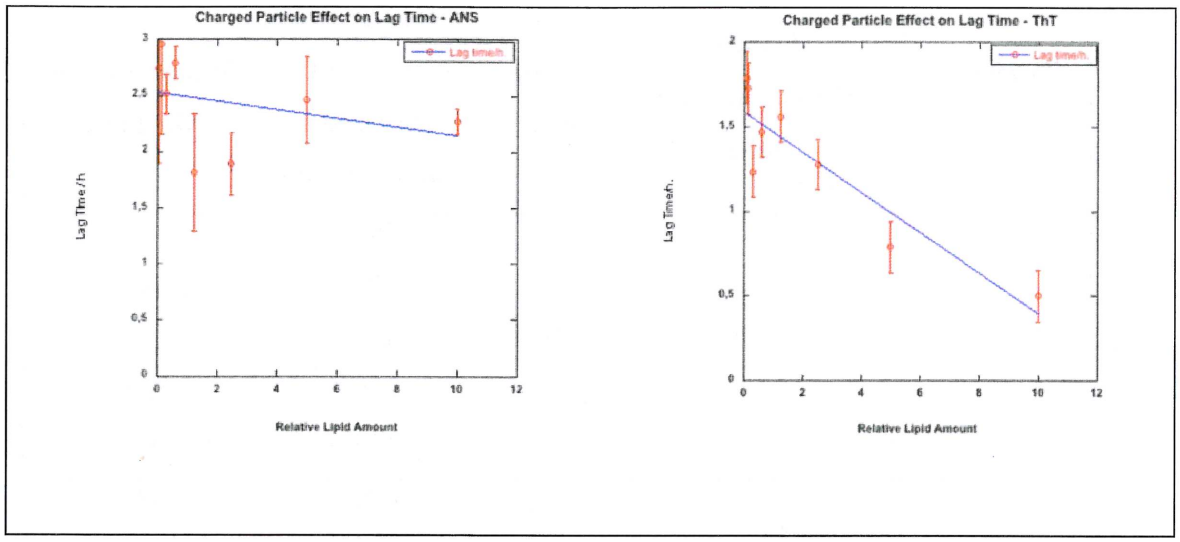


Figure 3.9 Charged Particle Dependence of Lag Time a) monitored by 1 μM ANS b) monitored by 20 μM ThT.

***Comparison between different lipid systems***

The same kinetics experiments (last 3 experiments in Table 3.3 and 3.4) were performed for different lipid systems, and we compared the anionic DOPC/CL vesicles to anionic DOPC/DOPS vesicles and zwitterionic DOPC vesicles. DOPS has one overall net negative charge. In the DOPC/DOPS lipid mixture, the charge was the same as in the DOPC/CL lipid vesicles, to see the effect of changing the lipid in the mixture. The experiments showed the same trends as observed for DOPC/CL vesicles in that the presence of anionic vesicles leads to an acceleration of the aggregation, as shown in Table 3.3 and Table 3.4.

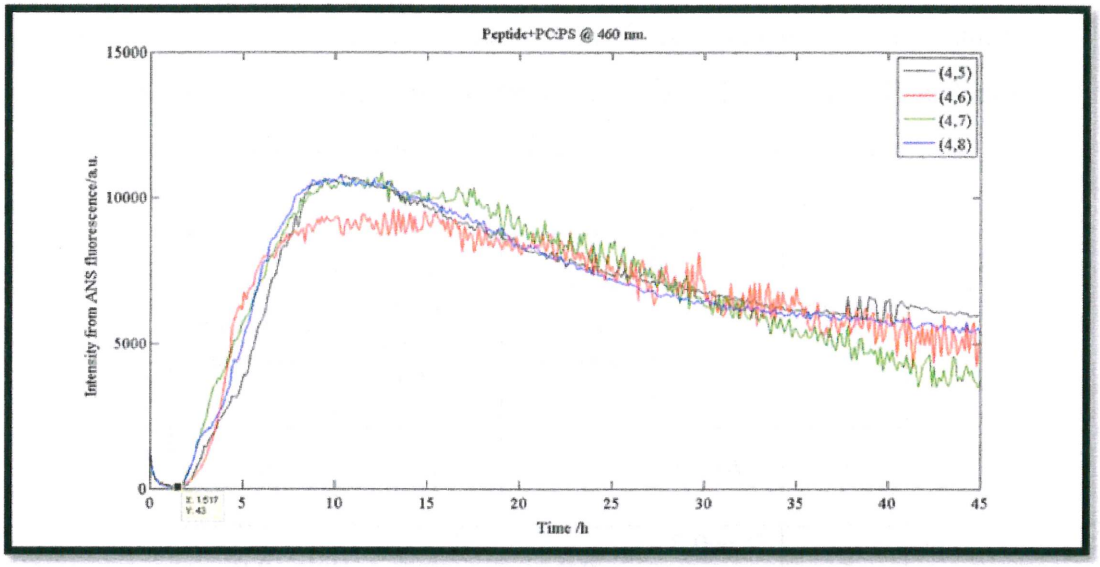


Figure 3.10 ANS Monitored Fibrillation Curve of 23 μM Peptide in presence of DOPC/DOPS (28 mol% DOPS) lipid vesicles at 460 nm. Peptide : Lipid ratio is 1:10. Different curves show different wells in the same plate.

Table 3.6-a Experimental Data from Plate Reader Measurements of 23 μM α-synuclein Fibrillation in Presence of 230 μM PC:PS Unilamellar Vesicles -ThT (Peptide:ThT = 1.15:1) Probe (Lag Time abbreviated as LT)

| Experiment Nr. | LT | LT (Peptide+PCPS)/ LT (Peptide + Buffer) | LT (PCCL)/LT (Peptide) (THT) |
|---|---|---|---|
| 5 | 2.9±0.3 | 0.6 | 2.0 |
| 6 | 4.6±0.4* | 0.4 | 1.2 |
| 7 | 1.8±0.4 | 0.3 | 0.4 |

Table 3.6b Experimental Data from Plate Reader Measurements of 23 μM α-synuclein Fibrillation in Presence of 230 μM PC:PS Unilamellar Vesicles -ANS (Peptide:ANS = 23:1) Probe (Lag Time abbreviated as LT)

| Experiment Nr. | LT | Lag time (ThT)/Lag time (ANS) | LT (Peptide+PCPS)/LT (Peptide + Buffer) | LT (PCCL)/LT(Peptide) ANS |
|---|---|---|---|---|
| 5 | 2.6±0.3 | 1.1 | 0.5 | 0.7 |
| 6 | 7.3±0.7 * | 0.9 | 0.6 | 0.8 |
| 7 | 2.2±0.4 | 0.8 | 0.3 | 0.4 |

From the data in Table 3.6, it is shown that the average of the ratio of ThT lag time to ANS lag time 0.93 h with a standard deviation of 0.12 h. Also in this case, intensity is lowered (Figure 3.10) compared to pure peptide fibrillation, all in all giving the same trend as PC:CL case. If we compare the lag time ratio of PCCL to pure peptide to the lag time ratio of PCPS to pure peptide experiments of especially from ANS, it is obvious that the lowering the lag times are similar for the different lipid systems.

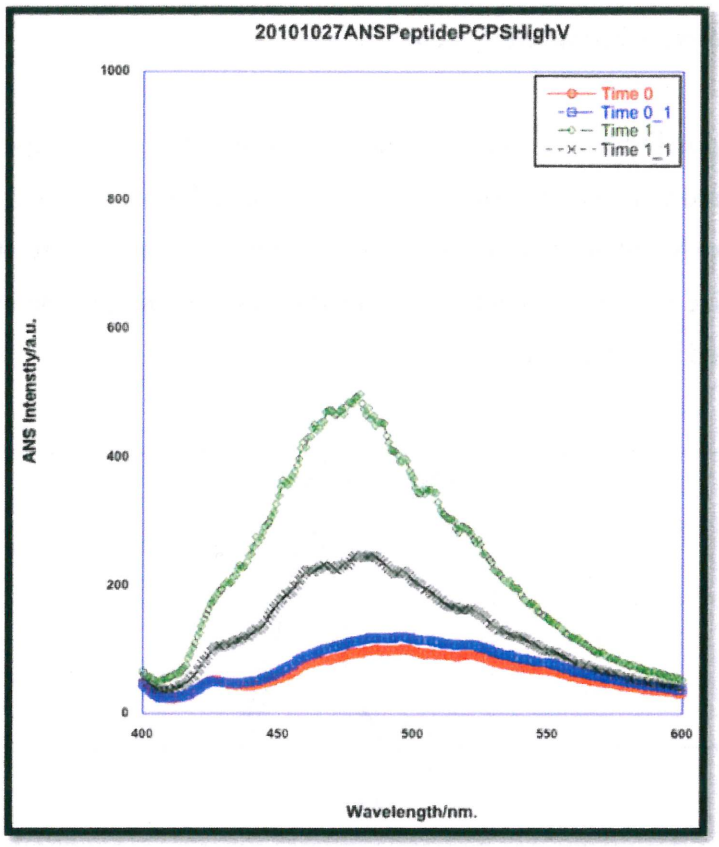


Figure 3.11 ANS spectrum of 2.3 μM Peptide incubated with 23 μM DOPC/DOPS in 3 μM ANS. Note that Time 0 is the initial measurement while Time 1 is the measurement at 45$^{th}$ h.

Figure 3.11 shows the wavelength and intensity shift upon fibrillation. The trend observed in the DOPC/CL system is also seen here; as time passes, there is a clear shift to the lower wavelengths from 500 nm to 470 nm. Here, scattering is less compared to pure peptide fibrils.

There are also few experiments performed using DOPC vesicles. However, for unknown reason, vesicle fusion was a major problem for the DOPC vesicles. As the system was not well controlled in terms of, e.g., accessible vesicle area, quantitative comparisons to the other lipid systems are not made.

***Other Parameters Affecting the System***

Regarding the possibility of fusion of lipid vesicles, in some of the experiments, DLS Zeta Sizer is used to detect the particle distribution in solution. Figure 3.12 shows the size distribution by intensity of PC:CL vesicles. This system is more stable and has more narrow size distribution compared to DOPC vesicles and give an average radius of 51.6 nm based on 3 experiments.

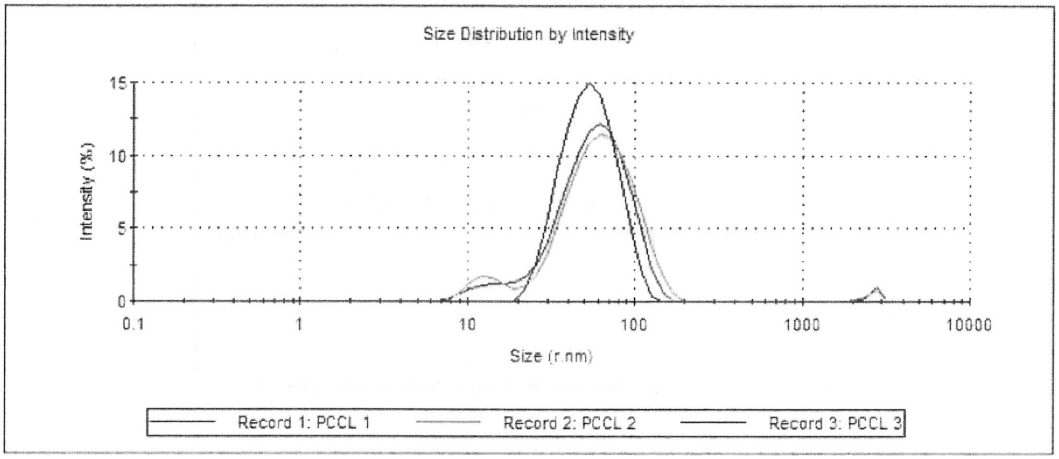


Figure 3.12 a) Size distribution of PC:CL Vesicles

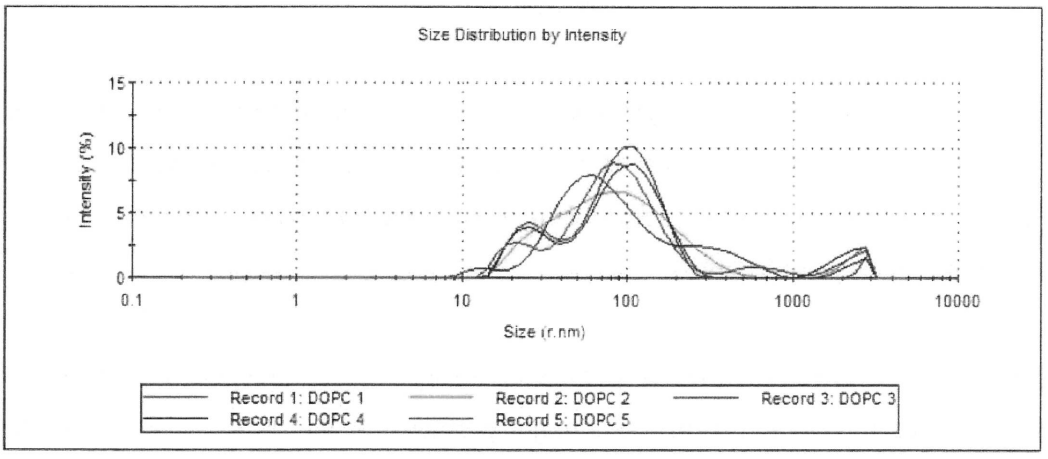


Figure 3.12 b) Size distribution of DOPC Vesicles

Also, the physical properties of the solution are important factors when stability of the system is concerned. pH is an extremely effective factor when it comes to proteins, changing their conformation quite easily. For amyloid aggregation, a small change in

pH can have a large effect on aggregation kinetics. A small change in pH may cause drastic changes in the system, resulting in lag time change.

That is why it is important to prepare all the solutions at same pH, in this case pH 5.5. When dispersed to prepare SUV's, lipid vesicles must be in buffer to preserve pH. However, it is always a good control to keep track of pH of lipid vesicles to avoid the inconsistency in the system. Luckily, lipid vesicles preserved the pH, right after sonication and after some hours during the experiment

## 3.3 Adsorption of α-synuclein fibrils on Surfaces

### 3.3.1 Adsorption Monitored by QCM-D

*Adsorption of Mature α-synuclein Fibrils*

In this work, adsorption of sonicated fibrils of α-synuclein to hydrophilic silica surfaces was studied. The question asked is whether the fibrils formed in the absence or presence of lipids has different surface properties that could affect how they adsorb to surfaces with different properties.

Figure 3.13 shows a typical adsorption curve of α-synuclein fibrils. Note that, after incubation of the fibrils, they had been sonicated until they get small enough to not to sediment. Then they have been diluted up to 4 μM to avoid the viscosity change when switching from buffer to fibril solution, which may actually lead to misinterpretations in modeling the system.

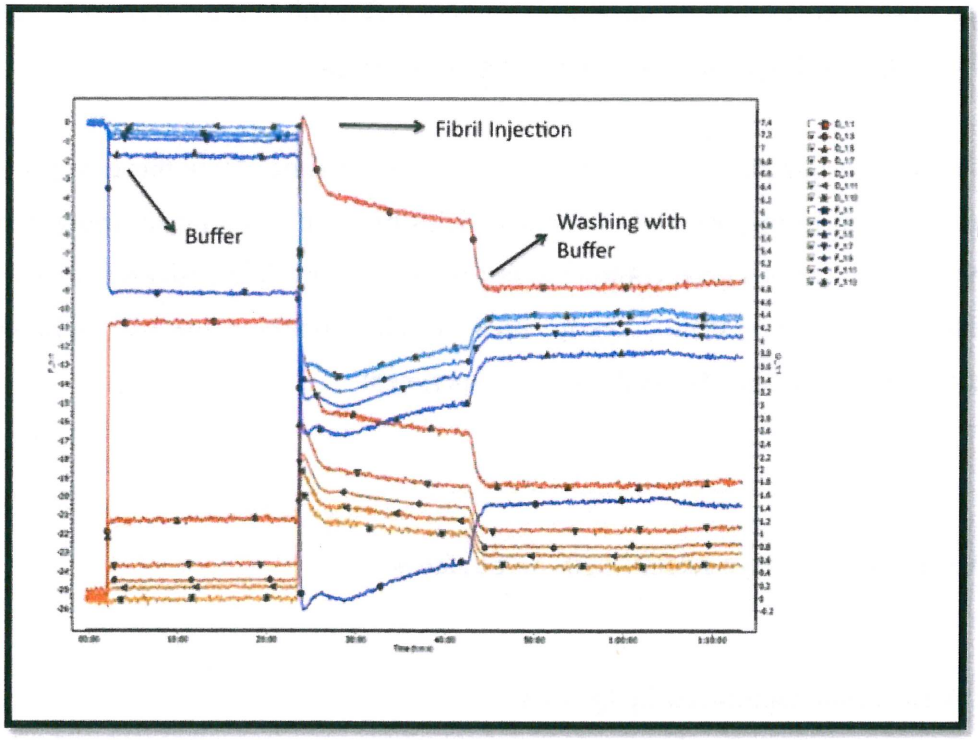


Figure 3.13 α-Synuclein Fibril Adsorption on Bare Silica Surface

As it can be seen from the adsorption graph, dissipation goes up above 1, which indicates that whatever adsorbed on the surface it adopts an extended structure and not collapsed. It is also noted that the different overtones do not overlay, which is again an indication that the adsorbed film is coupling quite substantial amounts of water. In this case, a viscoelastic model needs to be applied in the modeling of the data. Figure 3.14 shows only the fibril injection part of above figure, showing the accuracy of the model on our normalized data.

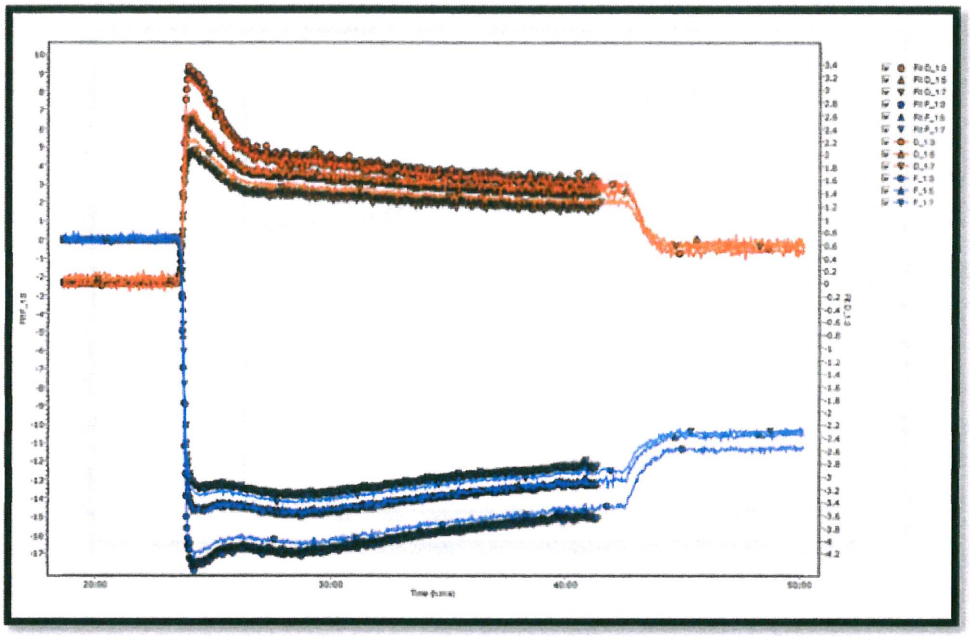

Figure 3.14 Viscoelastic model fit on alpha synuclein fibril adsorption

An average of 3 experiments at identical experimental conditions and peptide concentration gives an average adsorbed amount of 317.1 ng/cm$^2$ with a standard deviation of 13 ng/cm$^2$. In Figure 3.15, it can be seen how mass and viscosity changes upon injection of α-synuclein fibrils (based on the modeling). The mass change during the injection points out the structural changes during this time.

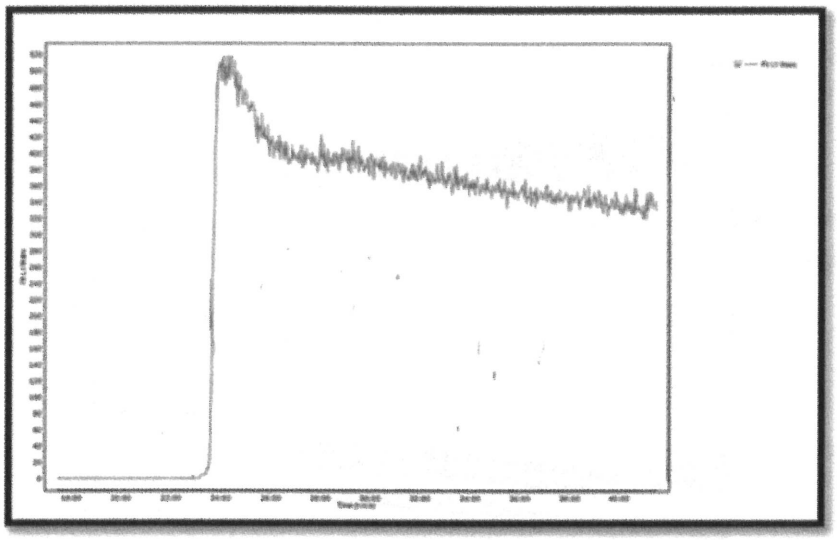

Figure 3.15 Mass change during alpha synuclein fibril injection.

In only one experiment, gold surface was used to have an idea about the adsorption to the hydrophobic surfaces. The adsorbed amount per area turned out to be quite the same as the hydrophilic surface and also giving a viscoelastic adsorption model.

***Adsorption of Mature α-synuclein Fibrils formed in Presence of DOPC:CL Vesicles***

Adsorption of α-synuclein fibrils incubated in presence of lipid vesicles to a hydrophilic silica surface was studied. The peptide concentration kept the same as in the experiments described above. In Figure 3.16, it can be seen that the adsorption pattern is almost the same as for pure peptide fibrils.

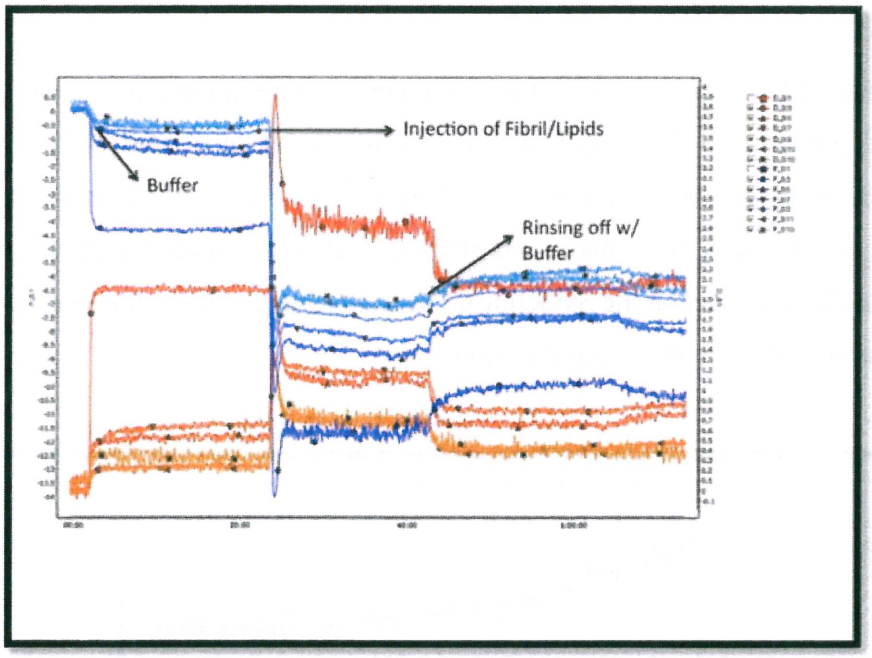


Figure 3.16 Alpha-Synuclein/PC:CL Fibril Adsorption on Bare Silica Surface

As it can be seen from the adsorption graph, dissipation goes up above 1, which again indicates that the adsorbed material is not lying flat as a condense film at the surface, and a viscoelastic model needs to be applied to model the data. Figure 3.17 shows only the fibril/lipid injection part of above figure, showing the accuracy of the model on our normalized data.

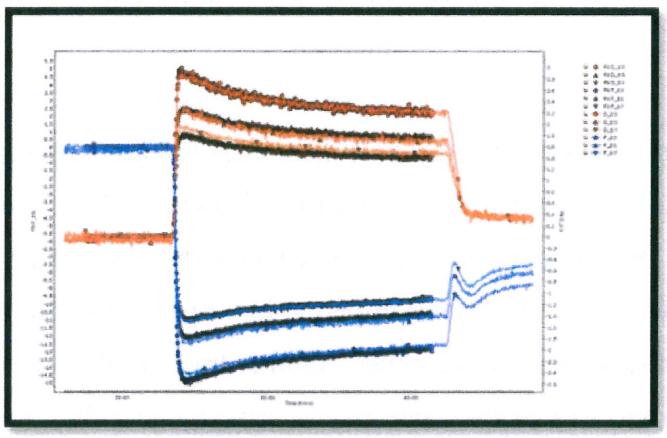

Figure 3.17 Viscoelastic model fit on alpha synuclein and PCCL Lipid Vesicles containing fibril adsorption

An average of 5 experiments with the same identical experimental conditions gives an adsorbed amount of 547.3 ng/cm$^2$ with a standard deviation of 168 ng/cm$^2$, which is larger compared to when the fibrils are formed in the absence of lipids. In Figure 3.18, it can be seen how mass and thickness changes upon injection of alpha-synuclein fibrils (based on the modeling). The mass change during the injection points out the structural changes during this time.

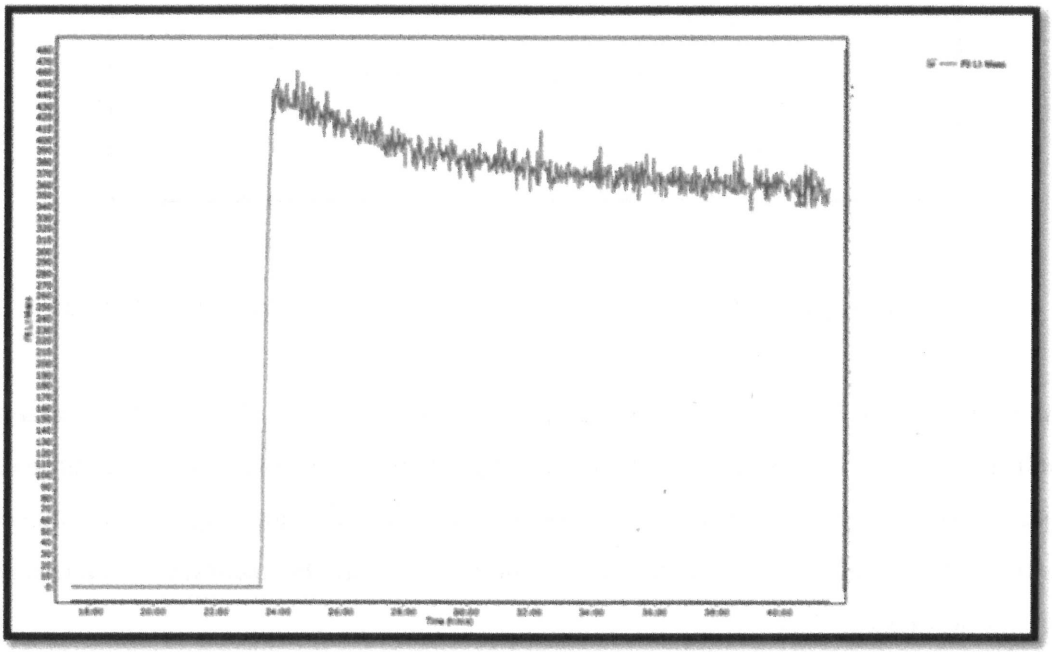

Figure 3.18 Mass change during alpha synuclein and PC:CL containing fibrils' injection.

It is important not to have free vesicles or monomers in injected sample. The peptide to lipid ratio had been chosen 1:1 to avoid excess amounts. In a control experiment, one fraction of the samples was centrifuged and the pellet was extracted after centrifugation. After this, fibrils were dispersed in buffer again, trying to preserve the same volume before extracting the pellet. Another fraction of the same samples was not centrifuged, and treated the same as the samples described in Figure 3.16. It turned out that the frequency and dissipation shifts are almost the same for both types of samples.

### 3.3.2 Adsorption Monitored by Ellipsometry

*Adsorption of Mature α-synuclein Fibrils*

Ellipsometry is a complementary method to QCM-D for comparing the mass adsorbed on a surface. Ellipsometry measurements were performed both on bare silica surface and silanized silica surface, method is described in [27]. Fibrillated α-synuclein peptide is sonicated until they get small enough to not to sediment. 500 µl of 40 µM sonicated fibrils are added inside of 5 ml cuvette, giving the same concentration as used in QCM-D experiments. Ellipsometry was performed for aggregates formed in the presence and absence of lipids, and for hydrophilic and hydrophobic silica surfaces. Each experiment was only performed once, and the results presented below are therefore considered preliminary.

Figure 3.19 shows the adsorption of α-synuclein fibrils on silica surface. Injection start from zero time and after t = 2500 s., rinsing takes place. It is shown that the adsorbed amount is really small. However, we have seen large adsorption and dissipation shift in the QCM-D. One possible explanation could be so that the adsorbed layer is quite dilute to give no change in refractive index.

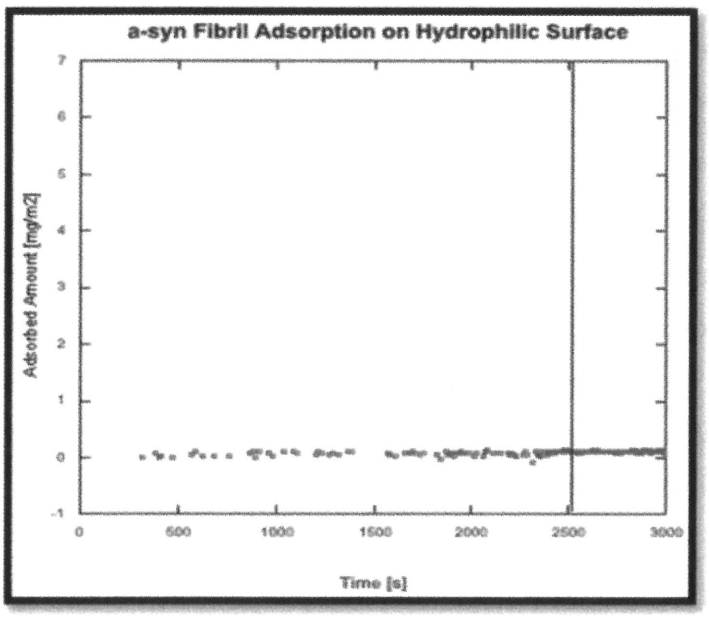


Figure 3.19 Fibril adsorption on Silica Surface

Figure 3.20 below shows the same sample added to a hydrophobic silanized surface. A small adsorption was detected. Note that the sample is injected at time 0, and after the solid line (t=7000 s), rinsing with buffer takes place.

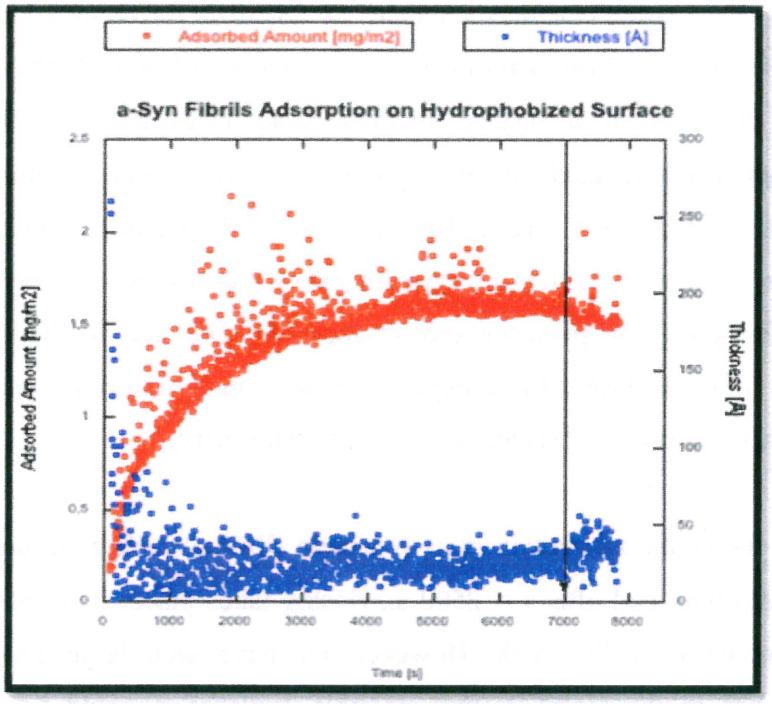


Figure 3.20 Fibril Adsorption on Silanized Surface

***Adsorption of Mature α-synuclein Fibrils formed in Presence of DOPC:CL Vesicles***

Alpha synuclein peptide incubated in the presence of DOPC:CL vesicles was studied to see the adsorption on two different surfaces. In these experiments, it was important to not to have excess free lipids and monomers in solution, and peptide to lipid ratio was chosen as 1:1. Figure 3.21 shows the adsorption behavior of this kind of fibrils onto hydrophilic bare silica surface. No fibrils adsorption was detected by ellipsometry. Note that after solid line (t = 3700 s.), rinsing takes place.

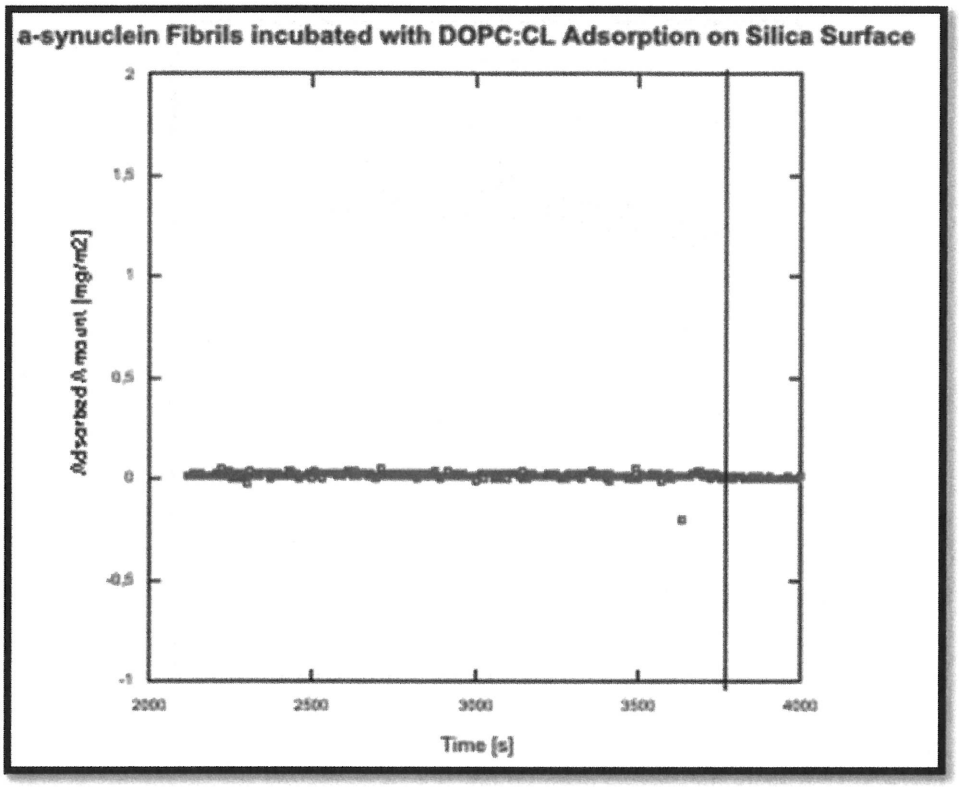


Figure 3.21 Fibrils incubated with DOPC:CL Adsorption on Silica Surface

Just as described for pure fibrils (Figure 3.19), the adsorption of fibrils formed in the presence of DOPC:CL vesicles was also studied on hydrophobic silanized surface (Figure 3.22). A comparison between Figure 3.20 and Figure 3.22 shows that the adsorbed amount is more or less the same but the thickness is almost ten times more in presence of DOPC:CL vesicles. That could be explained by a difference in aggregate properties or adsorption of free lipid vesicles.

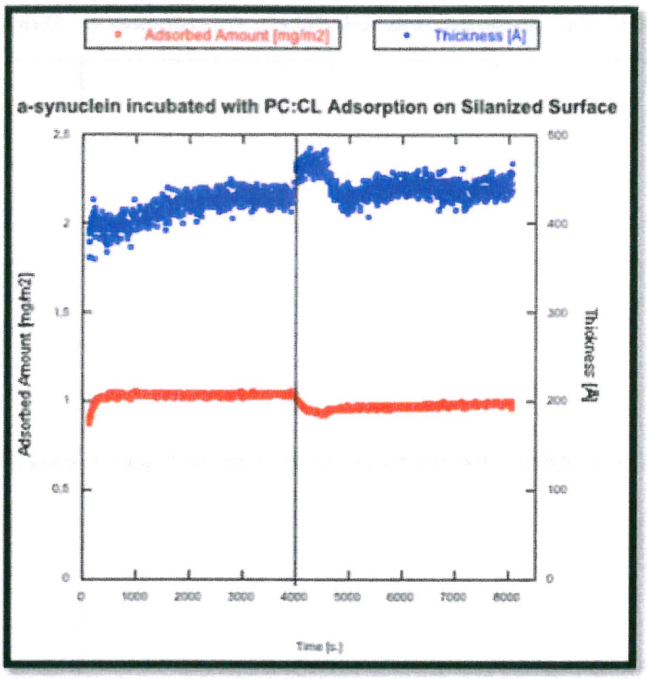


Figure 3.22 Fibrils incubated with DOPC:CL Adsorption on Silanized Surface

### 3.4 Experimental Considerations

It had been more practical to record the spectra directly in the wells on the plate using a plate reader in the fluorescence spectrometer, rather than moving the samples to a cuvette for the measurements at different time points. However, this set-up was not compatible with the instrumentation in hands. In the test experiments, the result turned out the same in each experiment, with or without protein and lipid contents, and it resulted in noisy spectra with low signal. The explanation for this was that there is only reflection from the transparent bottom of the plate that was recorded. In Fluostar Omega plate reader, the fluorescence is measured through the bottom whereas in Cary Eclipse fluorescence spectrometer equipped with plate holder, the fluorescence is measured from the top.

When silanizing QCM-D surfaces coated with $SiO_2$, cleaning process included sonication in 3 cycles, in total for 60 minutes. Unfortunately, the crystals got highly

damaged and worn off after that process, and therefore we were not able to perform comparable experiments simultaneously with QCM-D and ellipsometry.

## 4. DISCUSSION

The surface properties of α-synuclein fibrils incubated with or without lipids have been investigated using fluorescence spectroscopy techniques. Also the adsorption of those different aggregates has been studied using QCM-D and ellipsometry techniques.

### 4.1 Aggregation Kinetics of Pure α-synuclein Peptide

Understanding the aggregation kinetics of an amyloid system is important since it has a crucial role in neurodegenerative disease pathway. α-synuclein is a 140 amino acid protein that is present dopaminergic neurons and concentrated in the nerve terminals close to synaptic vesicles [28]. It is a "natively unfolded" protein and denatures under stress, affected by factors such as temperature and pH. It has a C-terminal region that is rather acidic and creates a net charge, which keeps the protein naturally unfolded. Another factor affecting the native state is the low overall hydrophobicity, typical for unstructured proteins. [29]

ThT is mostly used to detect the amyloid aggregates by increasing the intensity in presence of beta sheet structures, which are the hallmarks of fibrillation. ANS has an affinity for hydrophobic patches in the molecule, detecting the hydrophobicity of the sample investigated.

In the kinetic measurements, the same lag time was obtained with both ThT and ANS probes. These are typically sensitive to different properties in the system, the formation of stacked beta sheets and the presence of exposed hydrophobic patches, and it is an interesting observation that there is apparently a simultaneous change in these properties. A possible explanation of the trend could be such that fibrillation and

exposure of hydrophobic patches happen almost at the same time. Indeed, it has been claimed that when a natively unfolded protein starts to fold, the partially folded intermediate exposes its hydrophobic patches on the surface, which can alter the aggregation process [30]. Hoyer and coworkers observed the same trend by studying aliquots taken at different time points during incubation and binding ANS and ThT, recording the intensity afterwards [31]. They have suggested that there is no structural diversity of α-synuclein intermediate species under the same physical conditions during nucleation phase. However, what they did was not a continuous tracking of fluorescence intensity, which might cause complications since the kinetics data might be very scattered. There is a similar study in the literature by Bolognesi and coworkers [32], also using ANS on another amyloid peptide (Aβ). They have worked with ThT and ANS separately, which makes it difficult to track the fibrillation process. In our approach, simultaneous experiments produce highly reproducible data, which makes it easier to understand the correlation between ANS and ThT fluorescence.

### 4.2. Effect of Phospholipids on Aggregation Kinetics

It is important to investigate the effect of lipids on aggregation kinetics and on aggregate properties since one of the suggested mechanisms of Parkinson's disease emerges from interactions of the aggregating protein with membrane [33]. It has been claimed that membrane disrupts upon interaction of intermediate peptide species and lipids, leading to an increase in membrane permeability. It has also been shown that α-synuclein oligomeric species disrupt surface-deposited phospholipid vesicles. [34]

In this study, we have used model systems of mixed lipid vesicles. It is important to have cholesterol and lipids promote non-lamellar phases in the model membranes, since they are believed to exist in lipid rafts in membranes [35]. The focus of this study lies on the effect of charged lipids in the model membrane, since charge seems to play an important role in the interactions. Previous studies have shown that α-synuclein adsorbs to negatively charged lipid vesicles [36]. In our study, the lipid

systems used were mainly DOPC:CL and some experiments also performed with DOPC:DOPS.

The results revealed that, in the case of DOPC:CL, ANS and ThT indicate different lag times. However, the ThT-based lag time fluctuates a lot. If it would not be so, one could possibly say that hydrophobic patches are exposed faster than the fibrillation starts but we don't know since our ThT data is rather scattered.

The presence of lipid vesicles alters the fibrillation kinetics, as seen for both the DOPC:CL and the DOPC:DOPS systems. The effect of lipids on the α-synuclein aggregation kinetics is somewhat contradictory in the field. From the literature, it is clear that that retardation or the acceleration of α-synuclein aggregation is very sensitive to the lipid composition and relative compositions of lipid to peptide [7].

It is not predictable whether our system would have an acceleration or retardation in presence of self-assembled amphiphiles, as lipid vesicles. One also cannot say that lipid vesicles interfere with the aggregation, both can happen depending on the conditions of the solution. Lipid surfaces, though, can act as catalytic surfaces. Accumulation of peptide to the lipid surfaces could affect the system, lowering the energy barrier for nucleation and adsorbed peptides can start the association. Then one could also expect that the size of the vesicles is an important factor in this process. Size has an effect on the surface area of the vesicles, and a small size of vesicles may therefore accelerate the process more than large vesicles. On the other hand, amphiphiles, like lipids, might also protect hydrophobic patches, and thereby possibly retard fibrillation.

The relative concentration of vesicle to peptide also affects the lag time for the fibrillation. It was observed that the lag time has an inverse relationship with the concentration of the lipids. Similar effect was observed by Cabaleiro-Lago and coworkers in systems of amyloid proteins and positively charged nanoparticles [37]. Here, the charged particles were shown to have a dual effect on the half time of the fibrillation. Depending on the specific peptide:particle ratio, the kinetic effects vary from acceleration of the fibrillation process by reducing the lag phase at low particle

surface area in solution to inhibition of the fibrillation process at high particle surface area. The association of peptide on the interfaces can explain this trend. Note that the nanoparticles are different from self-assembled lipid vesicles in that their structure, size and shape is less likely to change upon the interaction with the aggregating protein.

Note that after fibrillation it is likely not appropriate to talk about unilamellar vesicles, as these likely fused or possibly associated with the protein.

The interaction between α-synuclein and the lipid vesicles can origin from hydrophobic and electrostatic interactions. In understanding the latter, it is important to consider the protein charge. The pI of α-synuclein is 4.7 [38], and at our conditions (pH 5.5) the C-terminal region still contains some negative charges. Still, the N-terminal part contains some positive charge, and association with negatively charges vesicles can therefore occur. It has also been proposed that binding of the vesicles promote alpha helix formation of the α-synuclein N terminus.

### 4.3. Effect of Phospholipids on the Hydrophobicity along the Aggregation Process

In the amyloid field, most of the studies have been performed assuming that the intermediate structures are defined and they can be isolated. However, it can be misleading to base experiments on the isolated intermediate structures since they might not be defined well; even though the aggregation kinetics are reproducible.

In our case, instead of trying to isolate the intermediate species, we have tried to carry out an on-line measuring process with different fluorescent techniques. In the end, it was proposed from the ANS fluorescence that the surface hydrophobicity increased in a correlation with the fibrillation process, giving no intensity of the monomers in the beginning.

When comparing a pure peptide system with the peptide system including lipid vesicles, it is seen that initially pure peptide system is more polar than the case when

lipids are present. There is a clear decrease in the intensity of fluorescence spectra when lipids are present in the system upon fibrillation. One possible reason could be such that lipids cover the accessible surface area for ANS, therefore having less surfaces open for ANS binding when lipids are present. Another reason could be different shape of aggregates with less accessible area. Still, those are not enough indications for conclusion since it needs to be confirmed by other techniques.

There is also a small difference in the wavelength shift between the aggregates formed in the presence and absence of lipids, which might again imply that aggregates have different properties.

There may be confusion about ANS' binding preference. It could either associate to the lipid bilayer and give again hydrophobicity indication or it could bind the hydrophobic surfaces of protein aggregate. First of all, ANS has a slight negative charge, which will disable the molecule to associate with anionic lipid vesicles. Indeed, the idea is confirmed with the control experiments, giving no trace of shift or intensity for DOPC:CL system. This leads to a conclusion that what detected during peptide incubated in presence of lipids experiments is the change in the protein aggregates. On the other hand, when ANS is added to the systems containing PC vesicles, after some time a shift in intensity was observed. One may say that, there is no charge repulsion between the probe and vesicles, leading to partitioning of ANS to the lipid bilayer. Unfortunately, these systems were not further investigated – which was not actually the concern of the study.

### 4.4. Adsorption to the Surfaces

QCM-D and ellipsometry are two complementary techniques that give quantitative information about the adsorption of the molecules to the surfaces. It is possible to model the outcoming data giving the adsorption amount and the thickness of the layer adsorbed. Moreover, monitoring the dissipation with QCM-D gives an idea about the structure of adsorbed layer of the substance.

In our work, we mostly worked on silica surfaces, known to be hydrophilic and slightly negative. By just looking at QCM-D frequency and dissipation shift on silica surfaces, we can say that the adsorbed layer of α-synuclein fibrils incubated with or without lipids are not compact but rather extended structures that couples some amount of buffer. The viscoelastic model used gives a relatively good fit to the data. The quantitative result is that there is a difference between adsorbed amount of pure α-synuclein fibrils and α-synuclein fibrils in presence of lipids.

Previous studies show that QCM-D measures the mass uptake coupled with buffer [39, 40]. Indeed in our case, we have observed that on the same type of silica surface the adsorption is not detectable by ellipsometry. It is first important to note that the roughness and the layer thickness is not the same for the surfaces used for the different techniques. It is also possible that the results can be explained by that the different surface techniques used indeed monitors slightly different properties of the system. From the QCM-D measurements, it is known that we have an extended peptide layer with a lot of coupled buffer, we can have a speculate that the adsorbed layer is so dilute in peptide that it does not give a significant difference in refractive index to detect in the ellipsometry measurements. However, ellipsometry data was not reproduced and therefore a definite conclusion cannot be made. Still, it is a clear observation for both pure peptide fibrils and peptide fibrils incubated with lipid vesicles, that they form extended structures when adsorbed to hydrophilic surfaces and couple a significant amount of buffer with them.

However, the adsorption is different in the case of hydrophobized silica. When comparing adsorption to the hydrophilic silica, it is concluded that the adsorbed amount is larger for fibrils formed in the presence of lipids. Only one set of experiments was done for the adsorption of fibrils to the hydrophobized silica surface, and these data needs to be reproduced. Still the observations made are interesting, and the adsorbed amount is slightly higher for pure peptide fibrils compared to fibrils formed in the presence of lipids. A possible explanation for these observations could be so that the aggregates formed in presence of lipids are less hydrophobic than pure peptide fibrils, thus giving higher adsorption to hydrophilic surfaces and lower adsorption to hydrophobic surfaces. This would also agree with the lowering of ANS

binding to lipid-peptide aggregates, as proposed above. Still, these results could clearly be explained also in other ways, and to draw definitive conclusions, further studies (using complementary techniques and more control experiments) are needed. In the comparison between ellipsometry data, it is also noted that the thickness is almost 10 times more when aggregates are formed in presence of lipids. Relevant experiments with QCM-D and reproducible data with ellipsometry are needed to explain these observations.

The sample preparation for ellipsometry and QCM-D measurements is one aspect that need to be considered when interpreting the results. Since fibrillar aggregates are heterogeneous samples, a sonication procedure was used to prevent fibril sedimentation. This sonication makes fibrillar aggregates smaller but it remains as a question whether it lipid components are redispersed in the solution or not. Also the fibrillar aggregates need to be diluted almost ten times to get rid of the drastic effect of changing viscosity suddenly. Those two procedures might affect the samples, leading to complications in the experiments. Finally, from the present data, it is not possible to conclude that what is adsorbed is only fibrils, but the adsorbed amount may also include, e.g., free lipid vesicles. It is however noted that the adsorption occurs in one step. It is also noted that centrifuging the sample before sonication in order to get rid of the free protein monomers and lipid vesicles in solution did not give any significant difference in QCM-D adsorption.

## 5. CONCLUSIONS

- Aggregation of α-synuclein was simultaneously followed by both ANS and ThT fluorescence, and the results show that the lag time monitored by the different dyes are the same, indicating that fibrillation happens at the same time as the exposure of hydrophobic patches.

- When peptide is incubated with vesicles containing zwitterionic PC mixed with anionc CL or PS, the fibrillation process is accelerated as observed by ANS fluorescence.

- Different lipid mixtures have the same effect on aggregation kinetics, and both DOPC:CL and DOPC:DOPS accelerates the fibrillation process. The amount of charges was kept the same in the lipid systems investigated.

- The fibrillation lag time is inversely proportional to the relative lipid to peptide concentration. In other words, the more lipids present, the faster the fibrillation.

- On-line measurements with ANS show that the hydrophobicity increases as time passes, indicating that ANS binds to the surface exposed hydrophobic patches. This is also the case when lipids are involved in the aggregation process.

- When lipids are involved ANS also binds to the aggregates but with a less intensity and wavelength shift, indicating that the aggregates have different surface properties.

- Both pure peptide fibrils and peptide incubated in presence of lipids fibrils adsorb to silica surface in QCM-D and they form extended structures coupled with a lot of solvent. The results might seem contradictory with the results obtained by ellipsometry showing that the adsorption to the silica surface is very low. The differences might be explained by differences in the properties

of silica surfaces. Another possible explanation is that the adsorbed layer is extended and very dilute.

- Both lipid containing and pure peptide aggregates adsorb on the hydrophilic surfaces observed by QCM-D measurements, only lipid containing ones giving slightly more.

- Another notable observation is that peptide aggregates that contain lipids adsorb slightly less than pure peptide aggregates on hydrophobic surface, measured by ellipsometry. That might be explained by lipid containing aggregates being less hydrophobic than pure peptide aggregates as indicated by ANS binding as well, but data needs to be reproduced.

## REFERENCES


1. Fink, A.L., *The aggregation and fibrillation of alpha-synuclein.* Accounts of Chemical Research, 2006. **39**(9): p. 628-634.

2. Ruiperez, V., F. Darios, and B. Davletov, *Alpha-synuclein, lipids and Parkinson's disease.* Progress in Lipid Research, 2010. **49**(4): p. 420-428.

3. Welch, K. and J.Y. Yuan, *alpha-synuclein oligomerization: a role for lipids?* Trends in Neurosciences, 2003. **26**(10): p. 517-519.

4. Dobson, C.M., *Protein folding and misfolding.* Nature, 2003. **426**(6968): p. 884-890.

5. Murphy, R.M., *Kinetics of amyloid formation and membrane interaction with amyloidogenic proteins.* Biochimica Et Biophysica Acta-Biomembranes, 2007. **1768**(8): p. 1923-1934.

6. Rawicz, W., et al., *Effect of chain length and unsaturation on elasticity of lipid bilayers.* Biophysical Journal, 2000. **79**(1): p. 328-339.

7. Zhu, M., J. Li, and A.L. Fink, *The association of alpha-synuclein with membranes affects bilayer structure, stability, and fibril formation.* Journal of Biological Chemistry, 2003. **278**(41): p. 40186-40197.

8. Knight, J.D. and A.D. Miranker, *Phospholipid catalysis of diabetic amyloid assembly.* Journal of Molecular Biology, 2004. **341**(5): p. 1175-1187.

9. Gorbenko, G.P. and P.K.J. Kinnunen, *The role of lipid-protein interactions in amyloid-type protein fibril formation.* Chemistry and Physics of Lipids, 2006. **141**(1-2): p. 72-82.

10. Hamilton, R.L., *Lewy bodies in Alzheimer's disease: A neuropathological review of 145 cases using alpha-synuclein immunohistochemistry.* Brain Pathology, 2000. **10**(3): p. 378-384.

11. Davidson, W.S., et al., *Stabilization of alpha-synuclein secondary structure upon binding to synthetic membranes.* Journal of Biological Chemistry, 1998. **273**(16): p. 9443-9449.

12. Cole, N.B., et al., *Mitochondrial translocation of alpha-synuclein is promoted by intracellular acidification.* Experimental Cell Research, 2008. **314**(10): p. 2076-2089.

13. Jenner, P., *Oxidative stress in Parkinson's disease.* Annals of Neurology, 2003. **53**(Supplement 3): p. 26-38.

14. Spector, A.A. and M.A. Yorek, *MEMBRANE LIPID-COMPOSITION AND CELLULAR FUNCTION.* Journal of Lipid Research, 1985. **26**(9): p. 1015-1035.

15. Britannica, *Lipid Bilayer*, in *http://www.britannica.com/EBchecked/media/92240/Phospholipid-molecules-like-molecules-of-many-lipids-are-composed-of*. 2007.

16. Lipids, A.P., in *http://www.avantilipids.com/*.

17. Laboratory, U.o.V.A.I., *Epi-Fluorescence with Microscope*, in http://web.uvic.ca/ail/techniques/epi-fluorescence.html. 2005.

18. Hawe, A., M. Sutter, and W. Jiskoot, *Extrinsic fluorescent dyes as tools for protein characterization.* Pharmaceutical Research, 2008. **25**(7): p. 1487-1499.

19. Lakowicz, J.R., *Principles of Fluorescence Spectroscopy*. 3 ed. 2010, New York: Springer.

20. Bollag, D.M., *Gel-Filtration Chromatography*, in *Peptide Analysis Protocols*, B.M. Dunn, Editor. 1994, Humana Press, Inc: Totowa, NJ.

21. Q-Sense. *Q-Sense Sensors*. http://www.q-sense.com/q-sense-sensors 2010.

22. *Adsorption at Solid Surfaces / QCM-D*, in *Chalmers Soft Matter Graduate School*. 2010, Fredrik Höök: Hönö, Göteborg.

23. Liu, S.X. and J.T. Kim, *Application of Kevin-Voigt Model in Quantifying Whey Protein Adsorption on Polyethersulfone Using QCM-D.* Jala, 2009. **14**(4): p. 213-220.

24. Harland G. Tompkins, W.A.M., *Spectroscopic Ellipsometry and Reflectometry - A User's Guide*. 1999, New York: Wiley Interscience.

25. Bhak, G., et al., *Granular Assembly of alpha-Synuclein Leading to the Accelerated Amyloid Fibril Formation with Shear Stress.* Plos One, 2009. **4**(1).

26. Hellstrand, E., et al., *Amyloid beta-Protein Aggregation Produces Highly Reproducible Kinetic Data and Occurs by a Two-Phase Process.* Acs Chemical Neuroscience, 2010. **1**(1): p. 13-18.

27. Vandoolaeghe, P., F. Tiberg, and T. Nylander, *Interfacial behavior of cubic liquid crystalline nanoparticles at hydrophilic and hydrophobic surfaces.* Langmuir, 2006. **22**(22): p. 9169-9174.

28. Baba, M., et al., *Aggregation of alpha-synuclein in Lewy bodies of sporadic Parkinson's disease and dementia with lewy bodies.* American Journal of Pathology, 1998. **152**(4): p. 879-884.

29. Uversky, V.N., J.R. Gillespie, and A.L. Fink, *Why are "natively unfolded" proteins unstructured under physiologic conditions?* Proteins-Structure Function and Genetics, 2000. **41**(3): p. 415-427.

30. Uversky, V.N., J. Li, and A.L. Fink, *Evidence for a partially folded intermediate in alpha-synuclein fibril formation.* Journal of Biological Chemistry, 2001. **276**(14): p. 10737-10744.

31. Hoyer, W., et al., *Dependence of alpha-synuclein aggregate morphology on solution conditions.* Journal of Molecular Biology, 2002. **322**(2): p. 383-393.

32. Bolognesi, B., et al., *ANS Binding Reveals Common Features of Cytotoxic Amyloid Species.* Acs Chemical Biology, 2010. **5**(8): p. 735-740.

33. Furukawa, K., et al., *Plasma membrane ion permeability induced by mutant alpha-synuclein contributes to the degeneration of neural cells.* Journal of Neurochemistry, 2006. **97**(4): p. 1071-1077.

34. Volles, M.J., et al., *Vesicle permeabilization by protofibrillar alpha-synuclein: Implications for the pathogenesis and treatment of Parkinson's disease.* Biochemistry, 2001. **40**(26): p. 7812-7819.

35. McMullen, T.P.W., R. Lewis, and R.N. McElhaney, *Cholesterol-phospholipid interactions, the liquid-ordered phase and lipid rafts in model and biological membranes.* Current Opinion in Colloid & Interface Science, 2004. **8**(6): p. 459-468.

36. van Rooijen, B.D., M. Claessens, and V. Subramaniam, *Lipid bilayer disruption by oligomeric alpha-synuclein depends on bilayer charge and accessibility of the hydrophobic core.* Biochimica Et Biophysica Acta-Biomembranes, 2009. **1788**(6): p. 1271-1278.

37. Cabaleiro-Lago, C., et al., *Dual Effect of Amino Modified Polystyrene Nanoparticles on Amyloid beta Protein Fibrillation.* Acs Chemical Neuroscience, 2010. **1**(4): p. 279-287.

38. Fink, A.L., *Factors affecting the fibrillation of alpha-synuclein, a natively unfolded protein.* Misbehaving Proteins: Protein, ed. R.M. Murphy and A.M. Tsai. 2006: Springer. 265-285.

39. Ainalem, M.L., et al., *DNA Binding to Zwitterionic Model Membranes.* Langmuir, 2010. **26**(7): p. 4965-4976.

40. Hook, F., et al., *Variations in coupled water, viscoelastic properties, and film thickness of a Mefp-1 protein film during adsorption and cross-linking: A quartz crystal microbalance with dissipation monitoring, ellipsometry, and surface plasmon resonance study.* Analytical Chemistry, 2001. **73**(24): p. 5796-5804.